Old Dominion University Research Foundation

DEPARTMENT OF MATHEMATICS & STATISTICS
COLLEGE OF SCIENCES
OLD DOMINION UNIVERSITY
NORFOLK, VIRGINIA 23529

NOZZLE FLOW WITH VIBRATIONAL NONEQUILIBRIUM

By

Dr. J. H. Heinbockel, Principal Investigator

and

J. G. Landry, Graduate Research Assistant

Summary of Research (Final Report)
For the period ended August 31, 1995

Prepared for
National Aeronautics and Space Administration
Langley Research Center
Hampton, VA 23681-0001

Under
Research Grant NAG-1-1424
Dr. W.E. Meador, Technical Monitor
MD-High Energy Science Branch

August 1995

DEPARTMENT OF MATHEMATICS & STATISTICS
COLLEGE OF SCIENCES
OLD DOMINION UNIVERSITY
NORFOLK, VIRGINIA 23529

NOZZLE FLOW WITH VIBRATIONAL NONEQUILIBRIUM

By

Dr. J. H. Heinbockel, Principal Investigator

and

J. G. Landry, Graduate Research Assistant

Summary of Research (Final Report)
For the period ended August 31, 1995

Prepared for
National Aeronautics and Space Administration
Langley Research Center
Hampton, VA 23681-0001

Under
Research Grant NAG-1-1424
Dr. W.E. Meador, Technical Monitor
MD-High Energy Science Branch

Submitted by the
Old Dominion University Research Foundation
P.O. Box 6369
Norfolk, VA 23508

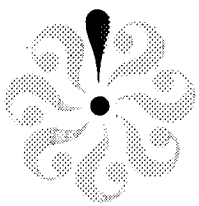

August 1995

FINAL PROGRESS REPORT
Research Grant NAG-1-1424
ODURF Grant Number 126613

by: J.H. Heinbockel, principal investigator
J.G. Landry, Graduate Research Assistant

NOZZLE FLOW WITH VIBRATIONAL NONEQUILIBRIUM

Introduction

The research of this project concerns the modeling and numerical solution of the coupled system of compressible Navier-Stokes equations in cylindrical coordinates under conditions of equilibrium thermodynamics and nonequilibrium thermodynamics.

The problem considered was the modeling a high temperature diatomic gas N_2 flowing through a converging-diverging high expansion nozzle. The problem was modeled in two ways. The first model uses a single temperature with variable specific heats as functions of this temperature. For the second model we assume that the various degrees of freedom all have a Boltzmann distribution and that there is a continuous redistribution of energy among the various degrees of freedom as the gas passes through the nozzle. Each degree of freedom is assumed to have its own temperature and consequently each system state can be characterized by these temperatures. This suggests the formulation of a second model with a vibrational degree of freedom along with a rotational-translation degree of freedom, each degree of freedom having its own temperature. Initially the vibrational degree of freedom is excited by heating the gas to a high temperature. As the high temperature gas passes through the nozzle throat there is a sudden drop in temperature along with a relaxation time for the vibrational degree of freedom to achieve equilibrium with the rotational-translation degree of freedom. That is, we assume that the temperature change upon passing through the throat is so great that the changes in the vibrational degree of freedom occur at a much slower pace and consequently lags behind the rotational-translational energy changes. This lag results in a finite relaxation time. In this context the term nonequilibrium is used to denote the fact that the energy content of the various degrees of freedom are characterized by two temperatures. We neglect any chemical reactions

which could also add nonequilibrium effects. We develop the energy equations for the nonequilibrium model from first principles.

The basic equations describing the nozzle flow can be represented in various forms., This is done in order to check the derivations with other sources, references [2],[3]. The final form which is solved numerically are scaled equations in a dimensionless form.

The two models to be compared are written in a weak conservative form using the symbols listed in the Appendix A. These derivations are from first principles and are consistent with other derivations as given in the references [18],[20]. The only difference in our derivation is that we use a more accurate representation for the relaxation time τ as developed by Meador, references [7],[28]. The viscosity is obtained from standard formulations based upon the Sutherland potential, reference [13]. The thermal conductivities are developed by employing a Eucken approximation, reference [30]. We calculate the steady state solution based upon an assumed laminar boundary layer and do not define a Mach number because of the dispersive sound speed. Our objective is to determine the velocity profiles and temperature profiles of both the translational-rotational and vibrational temperatures for the high expansion converging-diverging nozzle, which is defined in the Appendix B.

The resulting equations which model the nozzle flow can be expressed in various forms as indicated in the following sections. In most forms the resulting equations are a coupled system of nonlinear partial differential equations subject to certain boundary conditions. To solve the resulting coupled system of nonlinear partial differential equations, several numerical techniques were investigated (i) The explicit MacCormack method, reference [14], (ii) The explicit-implicit MacCormack method, reference [14], (iii) The method of operator splitting, reference [14],(iv) Factorization schemes and (v) The Steger-Warming scheme, reference [25].

Single Temperature Equations

For our first model we assume that there exists a single temperature T which characterizes the energy state of the system. The basic equations describing flow through a nozzle with cylindrical symmetry are given by (references [1],[3],[4],[12],[14], See also attached list of symbols in Appendix A.)

$$\text{Continuity} \qquad \frac{\partial}{\partial t}(r\varrho) + \frac{\partial}{\partial r}(r\varrho V_r) + \frac{\partial}{\partial z}(r\varrho V_z) = 0 \tag{1}$$

$$\text{Momentum} \qquad \frac{\partial}{\partial t}(r\varrho V_r) + \frac{\partial}{\partial r}(rT_{rr}) + \frac{\partial}{\partial z}(rT_{rz}) - T_{\theta\theta} = 0 \tag{2}$$

$$\frac{\partial}{\partial t}(r\varrho V_z) + \frac{\partial}{\partial r}(rT_{rz}) + \frac{\partial}{\partial z}(rT_{zz}) = 0 \tag{3}$$

$$\text{Energy} \qquad \frac{\partial}{\partial t}(re_t) + \frac{\partial}{\partial r}(r[(e_t + P)V_r - V_r\tau_{rr} - V_z\tau_{rz} + q_r])$$

$$+ \frac{\partial}{\partial z}(r[(e_t + P)V_z - V_r\tau_{zr} - V_z\tau_{zz} + q_z]) = 0 \tag{4}$$

where

$$q_r = -K\frac{\partial T}{\partial r}, \qquad q_z = -K\frac{\partial T}{\partial z} \tag{5}$$

$$T_{rr} = \varrho V_r^2 + P - \tau_{rr} \tag{6}$$

$$T_{rz} = \varrho V_r V_z - \tau_{rz} \tag{7}$$

$$T_{\theta\theta} = P - \tau_{\theta\theta} \tag{8}$$

$$T_{zz} = \varrho V_z^2 + P - \tau_{zz} \tag{9}$$

with the viscous stresses given by

$$\tau_{rr} = 2\eta\frac{\partial V_r}{\partial r} + \lambda\nabla\cdot\vec{V} \tag{10}$$

$$\tau_{zz} = 2\eta\frac{\partial V_z}{\partial z} + \lambda\nabla\cdot\vec{V} \tag{11}$$

$$\tau_{\theta\theta} = 2\eta\frac{V_r}{r} + \lambda\nabla\cdot\vec{V} \tag{12}$$

$$\tau_{rz} = \tau_{zr} = \eta\left(\frac{\partial V_z}{\partial r} + \frac{\partial V_r}{\partial z}\right) \tag{13}$$

$$\nabla\cdot\vec{V} = \frac{1}{r}\frac{\partial}{\partial r}(rV_r) + \frac{\partial V_z}{\partial z}. \tag{14}$$

The bulk viscosity is assumed to be zero, (Stoke's hypothesis), so that $\lambda = -2\eta/3$ and e_t is the total energy per unit volume and is given by

$$e_t = \varrho e + \frac{\varrho}{2}(V_r^2 + V_z^2), \tag{15}$$

where e is the internal energy per unit mass determined from the relation

$$de = C_v\, dT. \tag{16}$$

For a diatomic molecule the specific heats at constant volume and pressure are

$$C_v = C_{vrt} + C_{vv} \qquad \text{and} \qquad C_p = C_v + R \tag{17}$$

where R is the gas constant and $C_{vrt} = 5R/2$ is the specific heat at constant volume due to rotational and translational degrees of freedom and

$$C_{vv} = R\left(\frac{\phi}{T}\right)^2 \frac{e^{\phi/T}}{(e^{\phi/T}-1)^2}, \qquad \phi = \frac{h\nu}{k} \tag{18}$$

is the specific heat at constant volume due to the vibrational degree of freedom. The symbol ϕ denotes the characteristic vibrational temperature which is unique for each gas species. For example, the characteristic vibrational temperatures for O_2 is $\phi = 2270\,^\circ K$ and for N_2, $\phi = 3395\,^\circ K$. For small temperatures $C_v \approx 5R/2$ so that the vibrational degree of freedom only becomes excited when the temperature is on the order of ϕ.

Alternative Form for Energy Equation

The energy equation has the Cartesian tensor form

$$\frac{\partial e_t}{\partial t} + (e_t V_i)_{,i} = \frac{\partial Q}{\partial t} - q_{i,i} + \varrho b_i V_i + (-PV_i + \tau_{ij}V_j)_{,i} \tag{19}$$

where Q represents heat produced per unit volume, b_i represents body forces, and q_i represents heat transfer per unit volume. The momentum equation is written

$$\varrho\frac{\partial V_i}{\partial t} + \varrho V_{i,j}V_j = \varrho b_i - P_{,j}\delta_{ij} + \tau_{ij,j} \tag{20}$$

and when dotted with the velocity there results

$$\varrho V_i\frac{\partial V_i}{\partial t} + \varrho V_i V_j V_{i,j} = \varrho b_i V_i - V_i P_{,j}\delta_{ij} + V_i\tau_{ij,j} \tag{21}$$

or

$$\varrho\vec{V}\frac{D\vec{V}}{Dt} = \varrho\vec{b}\cdot\vec{V} - \vec{V}\cdot\nabla P + \vec{V}\cdot\nabla(\tau_{ij}). \tag{22}$$

Consider the identity

$$\begin{aligned}\varrho\frac{D}{Dt}(e_t/\varrho) &= \varrho\left[\frac{\partial}{\partial t}(e_t/\varrho) + \vec{V}\cdot\nabla(e_t/\varrho)\right] \\ &= \frac{\partial e_t}{\partial t} - \frac{e_t}{\varrho}\frac{\partial \varrho}{\partial t} + \varrho\vec{V}\cdot\nabla(e_t/\varrho)\end{aligned} \tag{23}$$

along with the continuity equation $\frac{\partial \varrho}{\partial t} = -\nabla(\varrho \vec{V})$ and the identity

$$\nabla \cdot (e_t \vec{V}) = \nabla(\varrho \vec{V} e_t/\varrho) = \nabla(e_t/\varrho)\varrho \vec{V} + \frac{e_t}{\varrho}\nabla(\varrho \vec{V}). \tag{24}$$

These results show that

$$\begin{aligned} \varrho \frac{D}{Dt}(e_t/\varrho) &= \frac{\partial e_t}{\partial t} + \frac{e_t}{\varrho}\nabla(\varrho \vec{V}) + \nabla(e_t \vec{V}) - \frac{e_t}{\varrho}\nabla(\varrho \vec{V}) \\ &= \frac{\partial e_t}{\partial t} + \nabla(\vec{V} e_t) = \frac{\partial e_t}{\partial t} + (e_t V_i)_{,i} \end{aligned} \tag{25}$$

Substituting equations (21) and (25) into equation (19) we obtain

$$\varrho \frac{De}{Dt} + \varrho \frac{D}{Dt}(V^2/2) = \frac{\partial Q}{\partial t} - \nabla \cdot \vec{q} + \varrho \frac{D}{Dt}(V^2/2) + \vec{V} \cdot \nabla P - \nabla(P\vec{V}) + (\tau_{ij} V_j)_{,i} - V_i \tau_{ij,j}. \tag{26}$$

Employing the identity

$$P \nabla \cdot \vec{V} = \nabla(P\vec{V}) - \vec{V} \cdot \nabla P$$

and defining the dissipation function

$$\Phi = (\tau_{ij} V_j)_{,i} - V_i \tau_{ij,j} \tag{27}$$

the equation (26) simplifies to the form

$$\varrho \frac{\partial e}{\partial t} + \varrho \vec{V} \cdot \nabla e + P \nabla \cdot \vec{V} + \nabla \vec{q} = \frac{\partial Q}{\partial t} + \Phi. \tag{28}$$

When $Q = 0$ there results the alternative form of the energy equation

$$\varrho \frac{\partial e}{\partial t} + \varrho \vec{V} \cdot \nabla e + P \nabla \cdot \vec{V} + \nabla \cdot \vec{q} - \Phi = 0, \tag{29}$$

where Φ is the dissipation function given by

$$\Phi = \nabla(\tau_{ij} V_j) - \vec{V} \cdot \nabla(\tau_{ij}) = (\tau_{ij} V_j)_{,i} - V_i \tau_{ij,j} \tag{30}$$

and can be represented as

$$\Phi = \eta \left[2(D_{11}^2 + D_{22}^2 + D_{33}^2) + (2D_{12})^2 + (2D_{13})^2 + (2D_{23})^2 \right] + \lambda \Theta^2 \tag{31}$$

where

$$D_{ij} = \frac{1}{2}(V_{i,j} + V_{j,i}) \qquad \text{and} \qquad \Theta = D_{ii}, \tag{32}$$

is the dilatation. In the above equations the summation convention for repeated indices is to be understood.

In cylindrical coordinates the dissipation function can be represented

$$\begin{aligned}\Phi =&\eta\left[2\left\{(\frac{\partial V_r}{\partial r})^2+(\frac{V_r}{r})^2+(\frac{\partial V_z}{\partial z})^2\right\}+\left(\frac{\partial V_r}{\partial z}+\frac{\partial V_z}{\partial r}\right)^2\right]+\\ &\lambda\left(\frac{\partial V_r}{\partial r}+\frac{V_r}{r}+\frac{\partial V_z}{\partial z}\right)^2\end{aligned} \tag{33}$$

In the limit as $r \to 0$ we use L'Hospital's rule that $\lim_{r\to 0} \frac{V_r}{r} = \frac{\partial V_r}{\partial r}$.

The internal energy per unit mass is given by

$$e = \int_{T_0}^{T} C_v\, dT = \int_{T_0}^{T}\left[\frac{5R}{2} + R(\phi/T)^2\frac{e^{\phi/T}}{(e^{\phi/T}-1)^2}\right] dT \tag{34}$$

which integrates to

$$e = \frac{5}{2}RT + \frac{R\phi}{e^{\phi/T}-1} + \text{Constant} \quad \text{and} \quad \frac{\partial e}{\partial T} = C_v. \tag{35}$$

The various quantities in the energy equation (29) are given by

$$\begin{aligned}\vec{V} &= V_r\,\hat{\mathbf{e}}_r + V_z\,\hat{\mathbf{e}}_z\\ \vec{q} &= q_r\,\hat{\mathbf{e}}_r + q_z\,\hat{\mathbf{e}}_z\\ e &= \frac{5}{2}RT + \frac{R\phi}{e^{\phi/T}-1}\\ \frac{\partial e}{\partial t} &= \frac{\partial e}{\partial T}\frac{\partial T}{\partial t} = C_v\frac{\partial T}{\partial t}\\ \varrho\vec{V}\cdot\nabla e &= \varrho V_r\frac{\partial e}{\partial r} + \varrho V_z\frac{\partial e}{\partial z}\\ \frac{\partial e}{\partial r} &= C_v\frac{\partial T}{\partial r} \qquad \text{and} \qquad \frac{\partial e}{\partial z} = C_v\frac{\partial T}{\partial z}\\ P\nabla\cdot\vec{V} &= P\left(\frac{\partial V_r}{\partial r}+\frac{V_r}{r}+\frac{\partial V_z}{\partial z}\right)\\ \nabla\cdot\vec{q} &= \frac{1}{r}\frac{\partial(rq_r)}{\partial r}+\frac{\partial q_z}{\partial z} = \frac{1}{r}\frac{\partial}{\partial r}(-rK\frac{\partial T}{\partial r})+\frac{\partial}{\partial z}(-K\frac{\partial T}{\partial z}).\end{aligned}$$

The thermal conductivity K is a function of temperature T so that

$$\nabla\cdot\vec{q} = -K\left(\frac{\partial^2 T}{\partial r^2}+\frac{1}{r}\frac{\partial T}{\partial r}+\frac{\partial^2 T}{\partial z^2}\right) - \frac{\partial K}{\partial T}\left[\left(\frac{\partial T}{\partial r}\right)^2+\left(\frac{\partial T}{\partial z}\right)^2\right]. \tag{36}$$

Vector Form For Equations of Motion

The weak conservative form for the basic equations of motion can be written as

$$\frac{\partial U'}{\partial t'} + \frac{1}{r^\alpha}\frac{\partial (rG')}{\partial r} + \frac{\partial F'}{\partial z} + \frac{1}{r^\alpha}H' = 0 \tag{37}$$

where $\alpha = 0$ is for two dimensional flow and $\alpha = 1$ is for axisymmetric flow, and

$$U' = \mathrm{col}(\varrho, \varrho V_r, \varrho V_z, e_t) \tag{38}$$

and

$$G' = \begin{bmatrix} \varrho V_r \\ \varrho V_r V_r + P - \tau_{rr} \\ \varrho V_r V_z - \tau_{rz} \\ (e_t + P)V_r - V_r\tau_{rr} - V_z\tau_{rz} + q_r \end{bmatrix} \tag{39}$$

with

$$F' = \begin{bmatrix} \varrho V_z \\ \varrho V_r V_z - \tau_{rz} \\ \varrho V_z V_z + P - \tau_{zz} \\ (e_t + P)V_z - V_r\tau_{rz} - V_z\tau_{zz} + q_z \end{bmatrix} \qquad H' = \begin{bmatrix} 0 \\ -P + \tau_{\theta\theta} \\ 0 \\ 0 \end{bmatrix}. \tag{40}$$

The above equations are to be solved over the computational domain $0 \le z \le b$ and $0 \le r \le f(z)$ where $f(z)$ defines the shape of the nozzle. We introduce the change of variables

$$x = z/b \qquad y = r/f(z), \qquad t = \frac{t'}{\frac{\varrho_0 b V_0}{P_0}} \tag{41}$$

and write the system of equations in the form

$$\frac{\partial U}{\partial t} + \frac{\partial E}{\partial x} + \frac{\partial F}{\partial y} + H = 0, \tag{42}$$

where

$$E = \frac{1}{b}F', \qquad F = \frac{1}{f}G' - \frac{yf'}{f}F', \qquad H = \frac{f'}{f}F' + \frac{1}{yf}(G' + H') \tag{43}$$

for $y \neq 0$. In the case $y = 0$ we use L'Hospital's rule and find that

$$H = \frac{f'}{f}F' + \frac{1}{f}\left(\frac{\partial G'}{\partial y} + \frac{\partial H'}{\partial y}\right). \tag{44}$$

We now introduce the scaled dimensionless variables

$$u_1 = \frac{\varrho}{\varrho_0}, \quad u_2 = \frac{\varrho V_r}{\varrho_0 V_0}, \quad u_3 = \frac{\varrho V_z}{\varrho_0 V_0}, \quad u_4 = \frac{e_t}{e_{t0}}, \tag{45}$$

and then employ a numerical method to solve the resulting dimensionless system.

Two Temperature Model

For our second model we assume a vibrational degree of freedom together with a combined rotational-translational degree of freedom. Each degree of freedom is assumed to follow a Boltzmann distribution and the energy content of each degree of freedom is characterized by temperatures T_v and T respectively. As the gas passes through the nozzle there is a certain finite relaxation time τ before the vibrational mode of excitation achieves equilibrium with the rotational-translational mode of excitation. Define the quantities:

n_i Population density of ith energy level

ϵ_i Energy per molecule of the ith level

$\dot{n}_i$ time rate of change of n_i due to V-T collisions

$\vec{q}_t$ Ordinary heat flux

$$\vec{q} = \vec{q}_{rr} + \vec{q}^*$$

where $\vec{q}_{rr}$ is the heat flux due to rotational energy

$\vec{q}^*$ Heat flux due to energy excitation of all energy levels

*Total energy from all energy levels

$$\vec{q}^* = \sum_i n_i \epsilon_i \vec{U}_i$$

where $\vec{U}_i = \vec{V}_i - \vec{V}$ is the diffusion velocity of molecule in state i

Φ The Dissipation function.

We construct a vibrational energy equation as follows. Let $\varrho e^* = \sum_i n_i \epsilon_i$ denote the total energy per unit volume from all excited states so that by integrating over the volume and surface of an arbitrary volume element we obtain

$$\frac{d}{dt}\int \varrho e^* \, dv = -\int_S \sum_i n_i \epsilon_i \vec{V}_i \cdot d\vec{S} + \sum_i \dot{n}_i \epsilon_i \, dv$$

where dv is a volume element and $d\vec{S}$ is an area element of the control volume and $\dot{n}$ are rate equations to be determined. Using the Gauss divergence theorem and interchanging the order of summation and integration there results

$$\begin{aligned} \frac{\partial}{\partial t}(\varrho e^*) + \sum_i \nabla(n_i \epsilon_i (\vec{U}_i + \vec{V})) &= \sum_i \dot{n}_i \epsilon_i \\ \frac{\partial}{\partial t}(\varrho e^*) + \nabla(\varrho e^* \vec{V}) &= \sum_i \left[\dot{n}_i \epsilon_i - \nabla(n_i \epsilon_i \vec{U}_i)\right]. \end{aligned} \tag{46}$$

Using the identities

$$\frac{D}{Dt}(\varrho e^*) = \frac{\partial(\varrho e^*)}{\partial t} + \vec{V}\cdot\nabla(\varrho e^*) + \nabla(\varrho e^*\vec{V}) - \varrho e^*\nabla\cdot\vec{V} - \vec{V}\cdot\nabla(\varrho e^*)$$

together with the continuity equation and

$$\frac{D}{Dt}(\varrho e^*) = \varrho\frac{De^*}{Dt} + e^*\frac{D\varrho}{Dt} = \varrho\frac{De^*}{Dt} - \varrho e^*\nabla\cdot\vec{V}$$

we write the vibrational energy equation as

$$\varrho\frac{De^*}{Dt} = \sum_i \dot{n}_i\epsilon_i - \nabla\vec{q}^*$$

where the rate equations are from Meador, et. al. [28], are given by

$$\frac{1}{\varrho}\sum_i \dot{n}_i\epsilon_i = \frac{e_e^* - e^*}{\tau}$$

where the subscript e denotes equilibrium. In the case where $*$ denotes the vibrational-vibrational energy mode (subscript v) we define

$$\lim_{\tau\to 0}\frac{e_V(T) - e_v(T_v)}{\tau} = C_{vv}\frac{DT_v}{Dt}, \qquad \lim_{\tau\to 0}\vec{q}_v = 0$$

so that the vibrational energy equation can be represented as

$$\varrho\frac{De_v}{Dt} = \varrho C_{vv}\frac{DT_v}{Dt} = \varrho\left[\frac{e_v(T) - e_v(T_v)}{\tau}\right] - \nabla\cdot\vec{q}_v. \tag{47}$$

The second energy equation is obtained by writing the energy equation (19) in the form

$$\varrho\frac{\partial}{\partial t}(e_{rt} + e_v) + \varrho\vec{V}\cdot\nabla(e_{rt} + e_v) + P\nabla\cdot\vec{V} + \nabla(\vec{q}_{rt} + \vec{q}_v) - \Phi + \varrho C_{vv}X - \varrho C_{vv}X = 0 \tag{48}$$

where

$$C_{vv}X = \frac{e_v(T) - e_v(T_v)}{\tau} \tag{49}$$

and then employing the vibrational equation (47) to obtain the coupled energy equations

$$\begin{aligned}\varrho\frac{\partial e_{rt}}{\partial t} + \varrho\vec{V}\cdot\nabla e_{rt} + P\nabla\cdot\vec{V} + \nabla\cdot\vec{q}_{rt} + \Phi + \varrho C_{vv}X &= 0\\ \varrho\frac{\partial e_v}{\partial t} + \varrho\vec{V}\cdot\nabla e_v + \nabla\cdot\vec{q}_v - \varrho C_{vv}X &= 0\end{aligned} \tag{50}$$

which reduces to the form

$$\begin{aligned}\frac{DT}{Dt} &= \frac{-1}{\varrho C_{rt}}\left(\nabla\cdot\vec{q}_{rt}+\Phi+P\nabla\cdot\vec{V}+\varrho C_{vv}X\right)\\ \frac{DT_v}{Dt} &= \frac{-1}{\varrho C_{vv}}\nabla\cdot\vec{q}_v+X\end{aligned} \tag{51}$$

where

$$e_v(T)=\int_{T_v}^{T} C_{vv}\,dT=\int_{T_v}^{T} R\left(\frac{\phi}{T}\right)^2\frac{e^{\phi/T}}{(e^{\phi/T}-1)^2}\,dT. \tag{52}$$

The integral in equation (52) is used to calculate

$$X=\frac{1}{C_{vv}\tau}(e_v(T)-e_v(T_v)).$$

Integration produces the result

$$X=\frac{T_v^2}{\phi\tau}\frac{1-e^{-\phi/T_v}}{1-e^{-\phi/T}}\left\{\exp\left[\phi\left(\frac{1}{T_v}-\frac{1}{T}\right)\right]-1\right\}. \tag{53}$$

The quantity $\varrho C_{vv}X=\frac{\varrho}{\tau}(e_v(T)-e_v(T_v))$ is thus a coupling term for energy between the vibrational and rotational-translational modes. The other terms in the coupled equations (51) are given by

$$C_v=C_{vrt}+C_{vv},\qquad C_{vrt}=5R/2,\qquad C_{vv}=R(\phi/T_v)^2\frac{e^{\phi/T_v}}{(e^{\phi/T_v}-1)^2} \tag{54}$$

$$e_{rt}=\frac{5}{2}RT \tag{55}$$

$$e_v=\int_{T_0}^{T_v} C_{vv}\,dT=\frac{R\phi}{e^{\phi/T_v}-1}+\text{constant} \tag{56}$$

$$X=\frac{1}{C_{vv}}(e_v(T)-e_v(T_v))$$

$$X=\frac{T_v^2}{\phi\tau}\left(\frac{1-e^{-\phi/T_v}}{1-e^{-\phi/T}}\right)\left\{\exp\left[\phi\left(\frac{1}{T_v}-\frac{1}{T}\right)\right]-1\right\} \tag{57}$$

$$\vec{q_{rt}}=-K_{rt}\nabla T \tag{58}$$

$$\vec{q_v}=-K_v\nabla T_v \tag{59}$$

$$K_{rt}=19\eta k/4m \tag{60}$$

$$K_v=\eta C_{vv} \tag{61}$$

$$\eta=\frac{c_1 g_c T^{3/2}}{T+c_2}\quad\text{Sutherland's formula} \tag{62}$$

$$c_1=(1.488)*2.16(10^{-8}),\quad g_c=5R/2,\quad c_2=184.0 \tag{63}$$

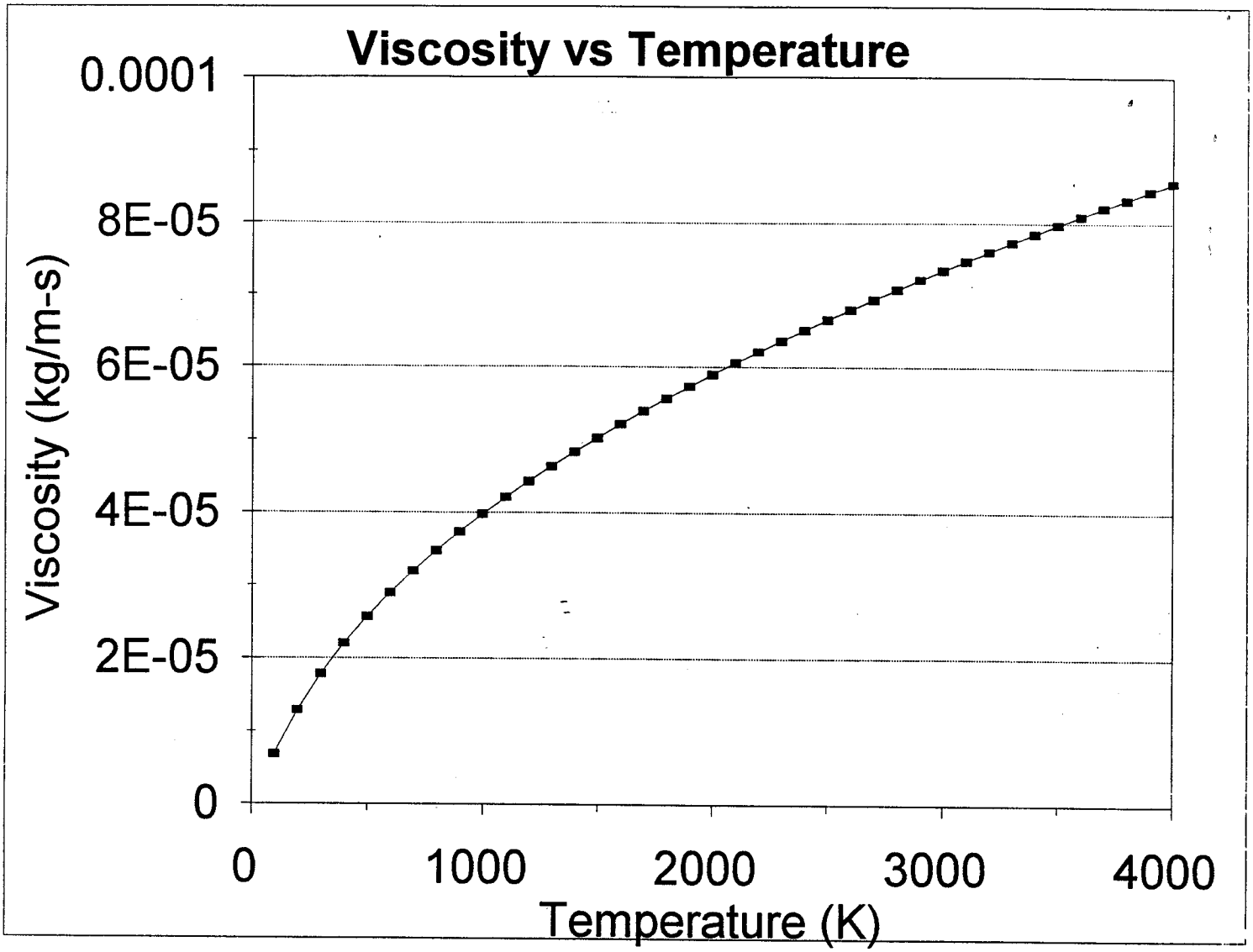

Figure 1. Viscosity vs Temperature from Sutherland potential

The Sutherland formula is illustrated in the figure 1 and depicts viscosity vs temperature. Also in the above equations we have used the Eucken approximation, reference [30], that the coefficient of self diffusion D satisfies the relation $\rho D = \eta$ to obtain the specific heats K_{rt} and K_v.

The divergence of the heat flux terms are then given by

$$\nabla \cdot \vec{q}_{rt} = -K_{rt}\left(\frac{\partial^2 T}{\partial r^2} + \frac{1}{r}\frac{\partial T}{\partial r} + \frac{\partial^2 T}{\partial z^2}\right) - \frac{\partial K_{rt}}{\partial T}\left[\left(\frac{\partial T}{\partial r}\right)^2 + \left(\frac{\partial T}{\partial z}\right)^2\right] \tag{64}$$

$$\nabla \cdot \vec{q}_{v} = -K_{v}\left(\frac{\partial^2 T_v}{\partial r^2} + \frac{1}{r}\frac{\partial T_v}{\partial r} + \frac{\partial^2 T_v}{\partial z^2}\right) - \frac{\partial K_{v}}{\partial T_v}\left[\left(\frac{\partial T_v}{\partial r}\right)^2 + \left(\frac{\partial T_v}{\partial z}\right)^2\right]. \tag{65}$$

For the pressure we assume an equation of state for an ideal gas $P = \rho RT$. Following Meador et.al. [28] the relaxation time τ for N_2 is taken as

$$P(atm)\tau = \frac{3.2188(10^{-12})}{I(T)\sinh(\phi/2T)}\left(\frac{T}{\theta}\right)^{1/2}\exp(-\xi/T) \tag{66}$$

where ϕ, θ, ξ are characteristic temperatures given by $\phi = 3395\,K$,$\theta = 3.2324(10^7)\,K$, $\xi = 95.9\,K$, and

$$I(T) = \int_{\frac{\phi+2\xi}{2T}}^{\infty}\left[1 + \left(1 + \frac{Tx}{\xi}\right)^{1/2}\right]^{1/3}\left(1 - e^{-2\varsigma_-}\right)\exp[-(x + \varsigma_+ - \varsigma_-)]\,dx \tag{67}$$

where

$$\varsigma_{\pm} = \left[\frac{16\theta T x}{27\phi^2}\left(1 \pm \frac{\phi}{2Tx}\right)\right]^{1/2}. \tag{68}$$

In the matrix form given by equation (42), we must replace the single temperature energy equation by energy equations associated with two temperatures.

The energy equations can also be written in a conservative form, and are added to the continuity and momentum equations. The equations are then scaled and solved similar to the one temperature model. The conservative form of the two temperature energy equations are obtained by letting $e_t = E_{rt} + E_v$ and writing

$$\begin{aligned}&\frac{\partial E_{rt}}{\partial t} + \frac{1}{r^\alpha}\frac{\partial}{\partial r}[r(E_{rt} + P)V_r - V_r\tau_{rr} - V_z\tau_{rz} + q_{rt}] + \\ &\frac{\partial}{\partial z}[(E_{rt} + P)V_z - V_r\tau_{rz} - V_z\tau_{zz} + q_{zrt}] + \frac{1}{r^\alpha}\varrho C_{vv}X = 0\end{aligned} \tag{69}$$

$$\frac{\partial E_v}{\partial t} + \frac{1}{r^\alpha}\frac{\partial}{\partial r}[rE_vV_r + q_{rv}] + \frac{\partial}{\partial z}[E_vV_z + q_{zv}] - \frac{1}{r^\alpha}\varrho C_{vv}X = 0 \tag{70}$$

where

$$E_{rt} = \frac{5}{2}\varrho RT + \frac{\varrho}{2}(V_r^2 + V_z^2) \tag{71}$$

$$E_v = \varrho R\Phi/(e^{\phi/T_v} - 1) \tag{72}$$

Both the single temperature and two temperature models have the weak conservative form given by the equations (42). The single temperature model has column vectors of dimension four, with while the two temperature model has column vectors of dimension five. For the two energy equation, nonequilibrium model, to facilitate the numerical method, the vector equations are written in the weak conservative form

$$\frac{\partial U_i}{\partial t} + \frac{1}{r}\frac{\partial (rG_i)}{\partial r} + \frac{\partial F_i}{\partial z} + \frac{1}{r}H_i = 0. \tag{73}$$

The continuity, momentum and energy equations then become

$$\frac{\partial \rho}{\partial t} + \frac{1}{r}\frac{\partial (r\rho V_r)}{\partial r} + \frac{\partial (\rho V_z)}{\partial z} = 0 \tag{74}$$

$$\frac{\partial (\rho V_r)}{\partial t} + \frac{1}{r}\frac{\partial (r(\rho V_r^2 + P - \tau_{rr}))}{\partial r} + \frac{\partial (\rho V_r V_z - \tau_{rz})}{\partial z} - \frac{1}{r}(P + \tau_{\theta\theta}) = 0 \tag{75}$$

$$\frac{\partial (\rho V_z)}{\partial t} + \frac{1}{r}\frac{\partial (r(\rho V_r V_z - \tau_{rz}))}{\partial r} + \frac{\partial (\rho V_z^2 + P - \tau_{zz})}{\partial z} = 0 \tag{76}$$

$$\frac{\partial (\rho e_{rt} + \frac{\rho}{2}(V_r^2 + V_z^2))}{\partial t} + \frac{1}{r}\frac{\partial (r((\rho e_{rt} + \frac{\rho}{2}(V_r^2 + V_z^2))V_r - V_z\tau_{rz} + q_{rtr}))}{\partial r} +$$

$$+ \frac{\partial ((\rho e_{rt} + \frac{\rho}{2}(V_r^2 + V_z^2))V_z - V_r\tau_{rz} - V_z\tau_{zz} + q_{rtz})}{\partial z} + \rho C_{vv} X = 0 \tag{77}$$

$$\frac{\partial (\rho e_v)}{\partial t} + \frac{1}{r}\frac{\partial (r(\rho e_v V_r + q_{vr}))}{\partial r} + \frac{\partial (\rho e_v V_z + q_{vz})}{\partial z} - \rho C_{vv} X = 0. \tag{78}$$

The total equilibrium energy, E_{rt}, is defined by

$$E_{rt} = \rho e_{rt} + \frac{\rho}{2}(V_r^2 + V_z^2), \tag{79}$$

and the total vibrational energy, E_v, by

$$E_v = \rho e_v. \tag{80}$$

The resulting set of equations can be represented as a vector equation

$$\frac{\partial U}{\partial t} + \frac{1}{r}\frac{\partial (rG)}{\partial r} + \frac{\partial F}{\partial z} + \frac{1}{r}H = 0, \tag{81}$$

where U, F, G, and H are vectors. The vector $U = \mathrm{col}(\rho,\ \rho V_r,\ \rho V_z,\ E_{rt},\ E_v)$, is the set of conservative variables.

The equations are now scaled by introducing the dimensionless variables defined by

$$
\begin{aligned}
r^* &= \frac{r}{\delta}, & \rho^* &= \frac{\rho}{\rho_0}, & e_{rt}^* &= \frac{e_{rt}}{V_0^2}, \\
z^* &= \frac{z}{L}, & V_r^* &= \frac{V_r}{\frac{V_0\delta}{L}}, & e_v^* &= \frac{e_v}{V_0^2}, \\
t^* &= \frac{t}{\frac{L}{V_0}}, & V_z^* &= \frac{V_z}{V_0}, & P^* &= \frac{P}{\rho_0 V_0^2}, \\
& & T^* &= \frac{T}{T_0}, & \eta^* &= \frac{\eta}{\eta_0}.
\end{aligned}
$$

where δ and L are characteristic lengths, V_0 is the characteristic velocity, ρ_0 is the characteristic density, and T_0 is a characteristic temperature. The characteristic viscosity, η_0, is the viscosity calculated at T_0. The Reynolds number, Re, is defined as the dimensionless combination of variables $Re = \frac{\rho_0 V_0 L}{\eta_0}$. The nozzle domain becomes $0 \leq r^* \leq \frac{f(Lz^*)}{\delta}$ and $0 \leq z^* \leq \frac{b}{L}$. The system of governing equations has the final scaled conservative form

$$\frac{\partial U^*}{\partial t^*} + \frac{1}{r^*}\frac{\partial (r^* G^*)}{\partial r^*} + \frac{\partial F^*}{\partial z^*} + \frac{1}{r*} H^* = 0, \tag{82}$$

where U^*, G^*, F^*, and H^* are the column vectors

$$U^* = \begin{bmatrix} \rho^* \\ \rho^* V_r^* \\ \rho^* V_z^* \\ E_{rt}^* \\ E_v^* \end{bmatrix} \tag{83}$$

$$G^* = \begin{bmatrix} \rho^* V_r^* \\ \rho^* V_r^* V_r^* + \frac{L^2}{\delta^2} P^* - \frac{L^2}{\delta^2}\frac{1}{Re}\tau_{rr}^* \\ \rho^* V_r^* V_z^* - \frac{L^2}{\delta^2}\frac{1}{Re}\tau_{rz}^* \\ (E_{rt}^* + P^*)V_r^* - V_r^*\frac{1}{Re}\tau_{rr}^* - \frac{L^2}{\delta^2} V_z^*\frac{1}{Re}\tau_{rz}^* + q_{rtr}^* \\ E_v^* V_r^* + q_{vr}^* \end{bmatrix} \tag{84}$$

$$F^* = \begin{bmatrix} \rho^* V_z^* \\ \rho^* V_r^* V_z^* - \frac{L^2}{\delta^2}\frac{1}{Re}\tau_{rz}^* \\ \rho^* V_z^* V_z^* + P^* - \frac{1}{Re}\tau_{zz}^* \\ (E_{rt}^* + P^*)V_z^* - V_r^*\frac{1}{Re}\tau_{rz}^* - V_z^*\frac{1}{Re}\tau_{zz}^* + q_{rtz}^* \\ E_v^* V_z^* + q_{vz}^* \end{bmatrix} \tag{85}$$

$$H^* = \begin{bmatrix} 0 \\ -\frac{L^2}{\delta^2} P^* + \frac{L^2}{\delta^2}\frac{1}{Re}\tau_{\theta\theta}^* \\ 0 \\ \frac{rL^*\rho^* C_{vv}^* X^*}{V_0^3} \\ -\frac{rL^*\rho^* C_{vv}^* X^*}{V_0^3} \end{bmatrix}. \tag{86}$$

The scaled equation of state is

$$P^* = \rho^* R T^* (\frac{T_0}{V_0^2}). \tag{87}$$

Finally, the nozzle is mapped to computational domain $0 \leq x \leq 1, 0 \leq y \leq 1$, which is the unit square, by employing the change of variables,

$$x = \frac{z^*}{b/L}, \quad y = \frac{r^*}{f(Lz^*)/\delta}, \tag{88}$$

The computational domain is then divided into 6 subregions for computational purposes. This computational domain is illustrated in the figure 2. The 6 subregions with nonuniform grid spacing requires a weighted representation of the derivatives for computational purposes. The final system of equations has the computational form

$$\frac{\partial U}{\partial t^*} + \frac{\partial E}{\partial x} + \frac{\partial F}{\partial y} + H = 0 \tag{89}$$

where

$$E = \frac{L}{b} F^*, \quad F = \frac{\delta}{f(bx)} G^* - \frac{Lyf'(bx)}{f(bx)} F^*, \tag{90}$$

$$H = \frac{Lf'(bx)}{f(bx)} F^* + \frac{\delta}{yf(bx)} (G^* + H^*), \quad U = U^*.$$

When y approaches zero, we obtain by L'Hospital's rule, the limit

$$lim_{y \to 0} \frac{\delta}{yf(xb)} (G^* + H^*) = \begin{bmatrix} 0 \\ -\frac{L^2}{\delta^2} \frac{\delta^2 \eta}{\rho f^2 Re} \frac{\partial^2 (\rho V_r)}{\partial y^2} \\ -\frac{L^2}{\delta^2} \frac{\delta}{fRe} \frac{\partial (\tau_{rx})}{\partial y} \\ -\frac{L^2}{\delta^2} \frac{\delta V_x}{fRe} \frac{\partial (\tau_{rx})}{\partial y} - \frac{L^2}{\delta^2} \frac{K_{rt} q_0 \delta^2}{f^2} \frac{\partial^2 T}{\partial y^2} + \varrho C_{vv} X \\ -\frac{L^2}{\delta^2} \frac{K_v q_0 \delta^2}{f^2} \frac{\partial^2 T_v}{\partial y^2} - \varrho C_{vv} X \end{bmatrix}. \tag{91}$$

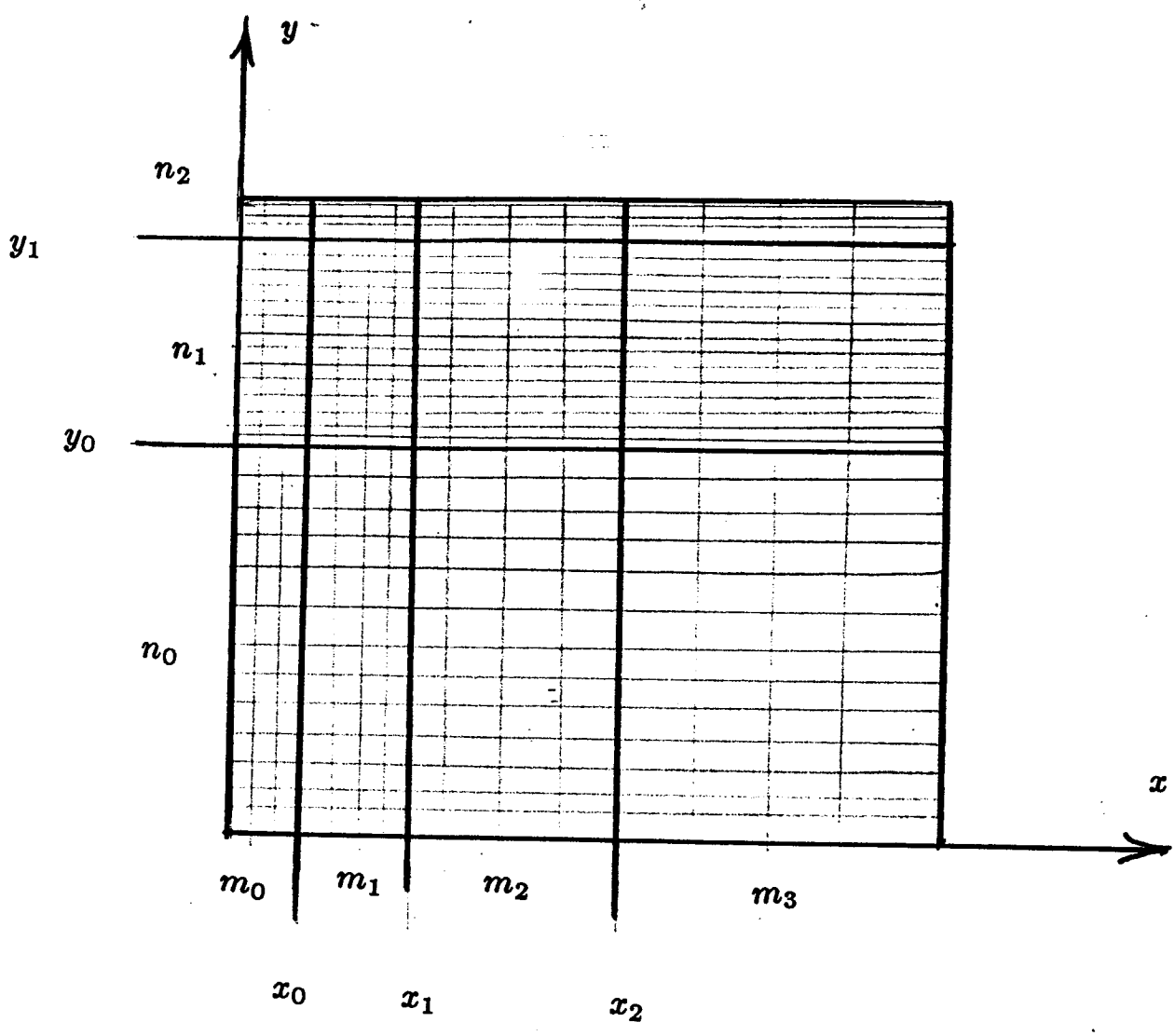

Figure 2. Computational Domain
m_0, m_1, m_2, m_3 are number of divisions of x-region.
n_0, n_1, n_2 are number of divisions of y-region.

Comparison with isentropic one-dimensional model

For comparison purposes we also assume an isentropic process and calculate the results for a one-dimensional flow through the nozzle in the z direction where the area of the nozzle

is a function of z. For an isentropic process we have

$$ds = \frac{dh - \frac{dP}{\varrho}}{T} = 0,$$

with $h = e + RT$, $e = \int_{T_0}^{T} C_v(T)\,dT$ and $dh = C_p\,dT$. Consequently,

$$ds = C_p \frac{dT}{T} - R\frac{dP}{P} = 0 \tag{92}$$

or

$$\int_{P_0}^{P} \frac{dP}{P} = \int_{T_0}^{T} \left[\frac{7}{2} + \left(\frac{\phi}{T}\right)^2 \frac{e^{\phi/T}}{(e^{\phi/T}-1)^2}\right] \frac{dT}{T}. \tag{93}$$

Let

$$V = \frac{1}{e^{\phi/T}-1}, \qquad dV = \frac{e^{\phi/T}}{(e^{\phi/T}-1)^2}\frac{\phi}{T^2}\,dT \tag{94}$$

and integrate by parts to obtain

$$\log P\,|_{P_0}^{P} = \frac{7}{2}\log T\,|_{T_0}^{T} + \frac{\phi}{T}\frac{1}{e^{\phi/T}-1}\,|_{T_0}^{T} + \int_{T_0}^{T} \frac{\phi}{T^2}\frac{1}{e^{\phi/T}-1}\,dT. \tag{95}$$

In the last integral, let $z = e^{\phi/T} - 1, dz = -e^{\phi/T}\frac{\phi}{T^2}dT$ so that

$$\int_{T_0}^{T} \frac{\phi}{T^2}\frac{1}{e^{\phi/T}-1}\,dT = -\int_{z_0}^{z} \frac{dz}{z(z+1)} = -\int_{z_0}^{z}\frac{dz}{z} + \int_{z_0}^{z}\frac{dz}{z+1}$$

and consequently

$$\int_{T_0}^{T} \frac{\phi}{T^2}\frac{1}{e^{\phi/T}-1}\,dT = \log\left(\frac{1-e^{-\phi/T_0}}{1-e^{-\phi/T}}\right). \tag{96}$$

Therefore, we can calculate the pressure ratio as

$$\frac{P}{P_0} = \left(\frac{T}{T_0}\right)^{7/2}\left(\frac{1-e^{-\phi/T_0}}{1-e^{-\phi/T}}\right)\exp\left(\frac{\phi/T}{e^{\phi/T}-1} - \frac{\phi/T_0}{e^{\phi/T_0}-1}\right). \tag{97}$$

Since $P = \varrho RT$ we can write

$$\frac{\varrho}{\varrho_0} = \left(\frac{T}{\phi}\frac{\phi}{T_0}\right)^{5/2}\left(\frac{1-e^{-\phi/T_0}}{1-e^{-\phi/T}}\right)\exp\left(\frac{\phi/T}{e^{\phi/T}-1} - \frac{\phi/T_0}{e^{\phi/T_0}-1}\right). \tag{98}$$

where ϕ/T_0 is treated as a parameter.

In one dimension the energy equation can be written

$$dh + V_z\,dV_z = 0 \quad \text{or} \quad C_p\,dT + V_z\,dV_z = 0. \tag{99}$$

Consequently, we may write

$$\int_{V_{z_0}}^{V_z} V_z \, dV_z = -\int_{T_0}^{T} C_p \, dT$$

which integrates to

$$V_z^2 - V_{z_0}^2 = 7R(T_0 - T) + 2R\phi\left(\frac{1}{e^{\phi/T_0}-1} - \frac{1}{e^{\phi/T}-1}\right). \tag{100}$$

By dividing by $a^2 = \gamma RT$, the local speed of sound, the one dimensional mach number can be represented

$$M^2 = \frac{V_{z_0}^2}{\gamma RT} + \frac{7}{\gamma}\left(\frac{T_0}{T} - 1\right) + \frac{2\phi}{\gamma T}\left(\frac{1}{e^{\phi/T_0}-1} - \frac{1}{e^{\phi/T}-1}\right) \tag{101}$$

with $M = V_z/a$. The mach number and one dimensional analysis is used to obtain an approximate solution to the more complicated two dimensional problem. Here

$$\gamma = \frac{C_p}{C_v} = \frac{7 + 2(\phi/T)^2 e^{\phi/T}(e^{\phi/T}-1)^{-2}}{5 + 2(\phi/T)^2 e^{\phi/T}(e^{\phi/T}-1)^{-2}}. \tag{102}$$

The one dimensional continuity equation is given by

$$AV_z\varrho = A^* V_z^* \varrho^* \tag{103}$$

where the $*$ quantities represent those values at the throat of the nozzle where $M = 1$. That is, set $M = 1$ in equation (101), then solve the equations (101)(102) simultaneously for the value of ϕ/T, treating ϕ/T_0 as a parameter. This calculated value of ϕ/T gives $T = T^*$ when $M = 1$ and consequently we can calculate the values of $P^*, \varrho^*, \gamma^*, V_z^*$ at this critical value of the temperature. The equation (103) can then be expressed in the following form involving the above critical parameters

$$\begin{aligned}
\frac{A}{A^*} &= \frac{V_z^* \varrho^*}{V_z \varrho} = \frac{\dfrac{V_z^*}{\sqrt{\gamma^* RT^*}}}{\dfrac{V_z}{\sqrt{\gamma RT}}} \frac{R\varrho^* T^*}{R\varrho T \frac{T^*}{T}} \\
\frac{A}{A^*} &= \frac{1}{M}\sqrt{\frac{\gamma^* T^*}{\gamma T}} \frac{P^*}{P\frac{T^*}{T}} = \frac{1}{M}\sqrt{\frac{\gamma^* T}{\gamma T^*}} \frac{P^*}{P} \\
\frac{A}{A^*} &= \frac{1}{M}\sqrt{\frac{\gamma^*}{\gamma}\frac{T}{\phi}\frac{\phi}{T^*}} \frac{P^*}{P_0}\frac{P_0}{P}.
\end{aligned} \tag{104}$$

Knowing the critical values $T^*, \gamma^*, P^*, A^*, V_z^*$ we can calculate the ratio T/ϕ as a function of A/A^* which is a function of z, with T_0/ϕ as a parameter. These one dimensional values are then used as starting values (initial conditions) for the solution of the two dimensional non-isentropic nozzle problem.

The figures 3,4,5,6 illustrate results from the above one-dimensional nozzle analysis.

Boundary conditions

Boundary conditions for both the model 1 and model 2 are similar. We state the boundary conditions for model 2. The steady solution of the governing equations is determined by the boundary conditions. In order to obtain a meaningful solution, boundary conditions must be applied that are not only applied correctly but are physically meaningful. The conditions are expressed in terms of the primitive variables $[\rho, V_r, V_z, T, T_v, P]$ and are converted to conservative variables when implemented numerically.

At the inflow boundary, the density and the translational-rotational temperature is held fixed at some initial values ρ_0 and T_0, respectively. This also means that the pressure is constant at the entrance. The vibrational temperature is assumed to be in equilibrium with the translational-rotational temperature and is also held constant at T_0. Gas is assumed to enter the nozzle parallel to the centerline, so the radial velocity is assumed to be zero. We set the flow to be subsonic at the inlet. An analysis of the flow characteristics of Euler's equations, reference [27], suggests that one boundary condition must be left free to change with the solution of the interior flow. To this end, the axial velocity is extrapolated from interior data. In the computational domain, this represents the condition $\frac{\partial V_z}{\partial x} = 0$.

At the far-field boundary, the flow is supersonic. All variables are extrapolated, or

$$\frac{\partial \rho}{\partial x} = \frac{\partial V_z}{\partial x} = \frac{\partial V_r}{\partial x} = \frac{\partial T}{\partial x} = \frac{\partial T_v}{\partial x} = 0. \tag{105}$$

Since

$$\frac{\partial P}{\partial x} = \rho R \frac{\partial T}{\partial x} + RT \frac{\partial \rho}{\partial x} = 0, \tag{106}$$

the pressure is also extrapolated.

The symmetry of the nozzle is used to specify the conditions along the centerline. Assuming that the quantities above the center axis are mirrored by those below, we have

$$\frac{\partial \rho}{\partial r} = \frac{\partial V_r}{\partial r} = \frac{\partial V_z}{\partial r} = \frac{\partial T}{\partial r} = \frac{\partial T_v}{\partial r} = \frac{\partial P}{\partial r} = 0. \tag{107}$$

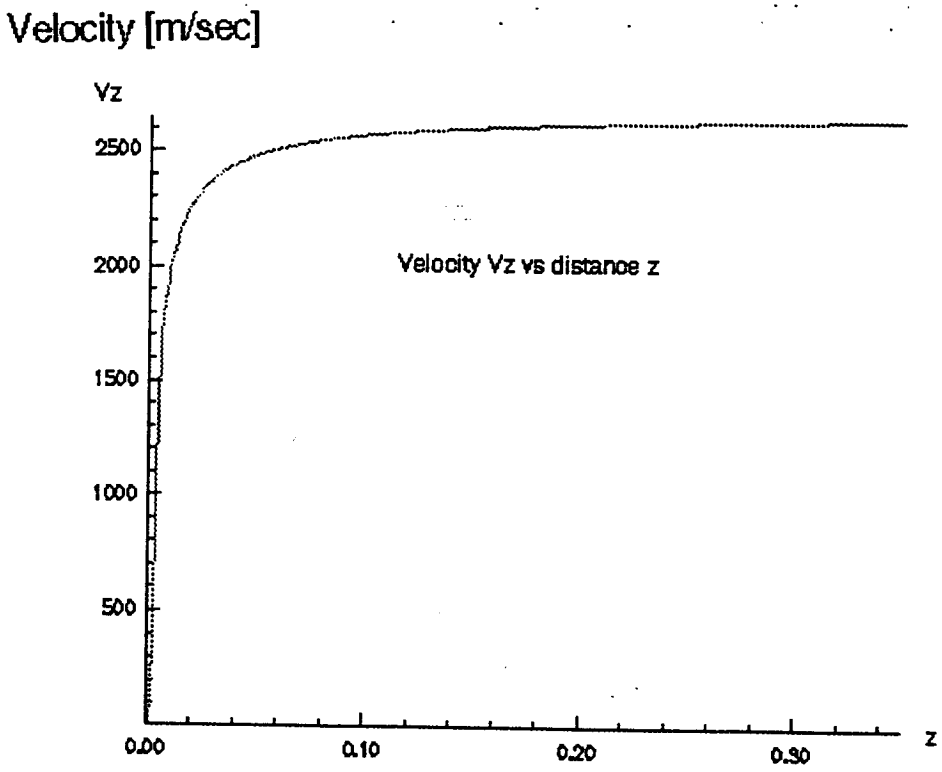

Figure 3. Velocity vs Distance

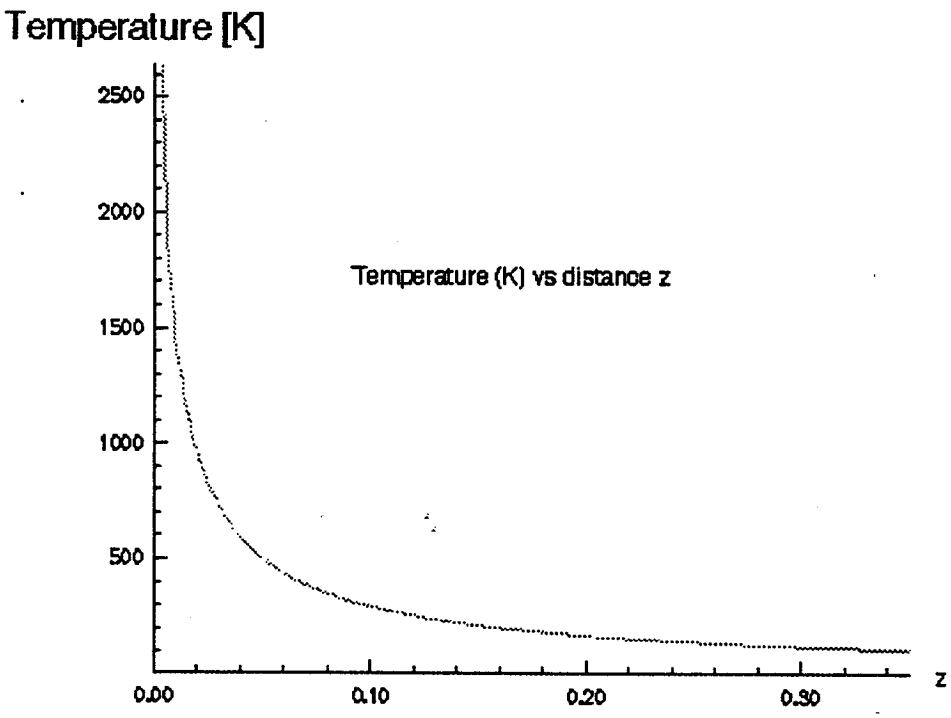

Figure 4. Temperature vs Distance

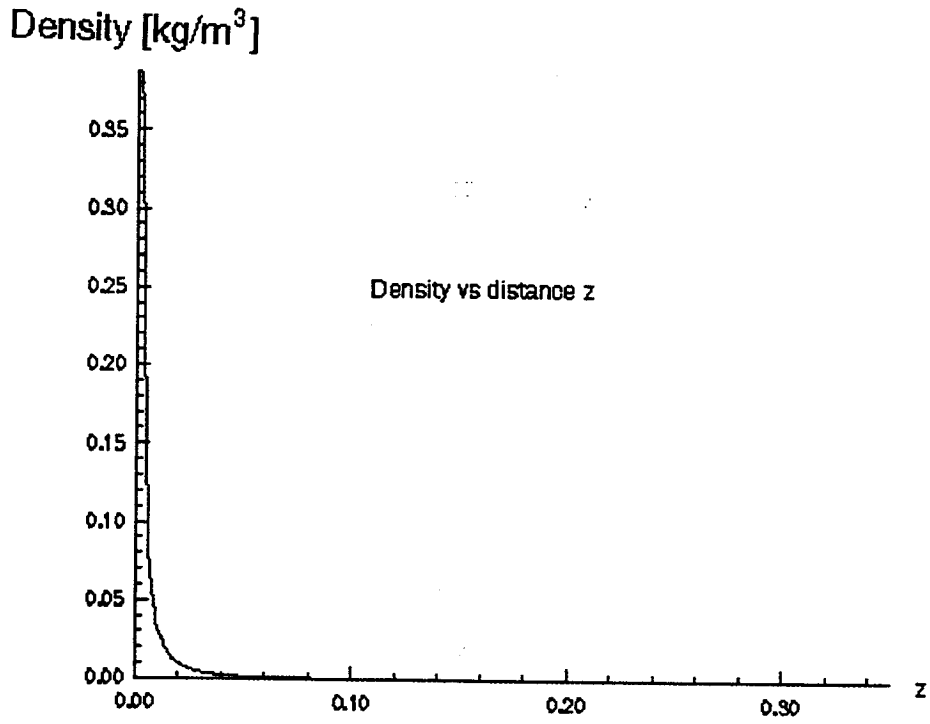

Figure 5. Density vs Distance

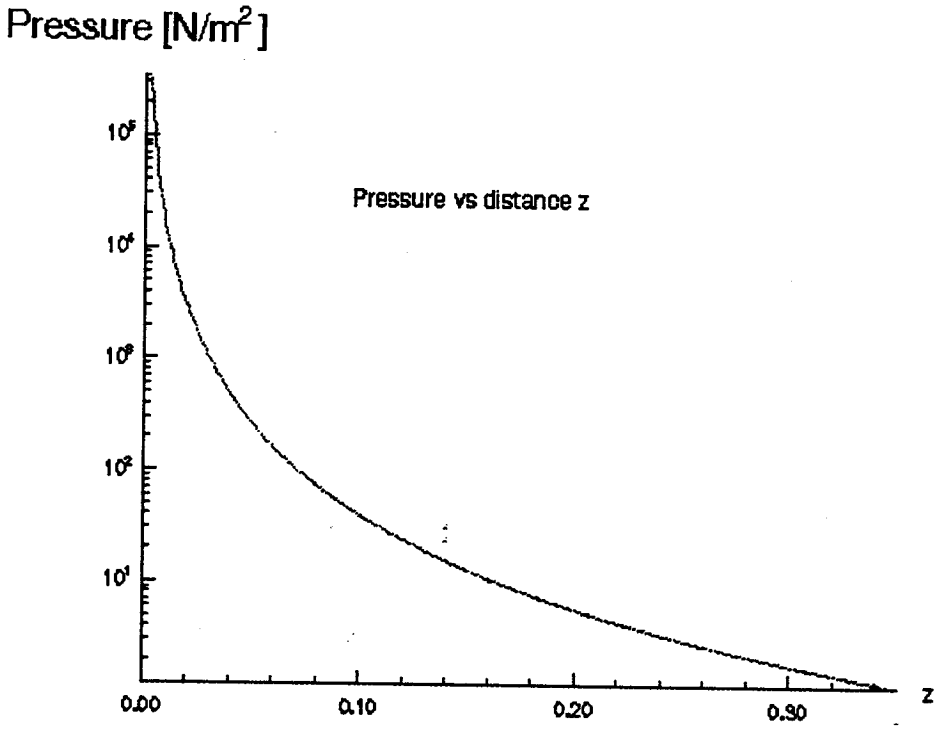

Figure 6. Pressure vs Distance

In the computational coordinates these conditions are simply

$$\frac{\partial \rho}{\partial y} = \frac{\partial V_r}{\partial y} = \frac{\partial V_z}{\partial y} = \frac{\partial T}{\partial y} = \frac{\partial T_v}{\partial y} = \frac{\partial P}{\partial y} = 0. \tag{108}$$

Furthermore, the radial velocity along the centerline is zero,

$$V_r = 0 \tag{109},$$

since the radial velocity at the centerline must flow equally in the positive and negative directions.

Lastly, boundary conditions on the nozzle wall are governed by the nozzle shape and the viscosity. Due to the viscosity, no-slip conditions are applied to the velocities at the wall boundaries,

$$V_r = V_z = 0. \tag{110}$$

The translational-rotational as well as the vibrational temperatures are extrapolated such that

$$\frac{\partial T}{\partial y} = \frac{\partial T_v}{\partial y} = 0. \tag{111}$$

The pressure gradient normal to the wall is assumed to be zero,

$$\frac{\partial P}{\partial n} = 0. \tag{112}$$

In computational coordinates this condition becomes

$$\frac{\partial P}{\partial n} = \frac{\partial P}{\partial x} - \frac{b}{f(xb)f'(xb)}(1 + (f')^2)\frac{\partial P}{\partial y} = 0. \tag{113}$$

The density on the boundary is then calculated using the ideal gas law evaluated on the boundary.

Initial conditions

The choice of initial conditions is also important. Values that are too far from the steady solution can make the numerical solution unstable. And of course, the closer the initial conditions are to the steady solution, the less time is required for convergence. To minimize the convergence time, the initial conditions are the steady state solution values obtained from the one-dimensional model previously discussed. The initial vibrational temperature is assumed in equilibrium with the translational-rotational temperature before the throat. After the throat, the vibrational-temperature is frozen at the centerline, throat translational-rotational temperature.

In summary, the initial flow conditions were set along the centerline from a one-dimensional analysis of the subsonic to supersonic nozzle flow for the nozzle defined in Appendix B. These conditions were then extrapolated to fill the remaining nozzle grid points. A no slip velocity condition was applied at the nozzle walls and symmetry conditions were assumed along the nozzle centerline. The exit pressure was lowered to a point such that shockless supersonic flow was maintained in the diverging half of the nozzle. These boundary and initial conditions are consistent with other researchers, references [1],[2],[3],[9],[17],[20]. However, the choice of appropriately well posed boundary conditions for internal flows appears to still be an open question, reference [17].

Numerical Methods

Various numerical methods can be used to solve the system given by the vector equation (42)

$$\frac{\partial U}{\partial t} + \frac{\partial E}{\partial x} + \frac{\partial F}{\partial y} + H = 0.$$

The following numerical techniques were applied to this equation.

The explicit MacCormack method

The explicit MacCormack method was developed in 1969 and is expressed by the algorithm:

Predictor:

$$\overline{U_{i,j}^{n+1}} = U_{i,j}^{n} - \frac{\Delta t}{\Delta x}(E_{i+1,j}^{n} - E_{i,j}^{n}) - \frac{\Delta t}{\Delta y}(F_{i,j+1}^{n} - F_{i,j}^{n}) - \Delta t H_{i,j}^{n}$$

Corrector:

$$U_{i,j}^{n+1} = \frac{1}{2}\left[U_{i,j}^{n} + \overline{U_{i,j}^{n+1}} - \frac{\Delta t}{\Delta x}(\overline{E_{i,j}^{n+1}} - \overline{E_{i-1,j}^{n+1}}) - \frac{\Delta t}{\Delta y}(\overline{F_{i,j+1}^{n+1}} - \overline{F_{i,j-1}^{n+1}}) - \Delta t \overline{H}_{i,j}^{n+1}\right]$$

where x_i, y_j is the (i,j) node point. This scheme is second order accurate provided the various derivatives are differenced correctly.

Operator Splitting

The weak conservative form for the equations (1) through (4) in terms of the computational coordinates x, y are given by

$$\frac{\partial U}{\partial t} + \frac{\partial E}{\partial x} + \frac{\partial F}{\partial y} + H = 0$$

where

$$E = F'/b, \qquad F = E'/b - F'yf'/f, \qquad H = H' + F'f'/f,$$

with

$$U = \mathrm{col}(r\varrho/r_0\varrho_0, r\varrho V_r/r_0\varrho_0 V_0, r\varrho V_z/r_0\varrho_0 V_0, re_t/r_0 e_{t0})$$

and

$$E' = \begin{bmatrix} \frac{r\varrho V_r}{r_0\varrho_0} \\ \frac{r(\varrho v_r^2 + P - \tau_{rr})}{r_0\varrho_0 V_0} \\ \frac{r(\varrho V_r V_z - \tau_{rz})}{r_0\varrho_0 V_0} \\ \frac{r((e_t+P)V_r - V_r\tau_{rr} - V_z\tau_{rz} + q_r}{)} r_0 e_{t0} \end{bmatrix},$$

$$F' = \begin{bmatrix} \frac{r\varrho V_z}{r_0\varrho_0} \\ \frac{r(\varrho V_r V_z - \tau_{rz})}{r_0\varrho_0 V_0} \\ \frac{r(\varrho V_z^2 + P - \tau_{zz})}{r_0\varrho_0 V_0} \\ \frac{r((e_t+P)V_z - V_r\tau_{rz} - V_z\tau_{zz} + q_z)}{r_0 e_{t0}} \end{bmatrix}, \quad H' = \begin{bmatrix} 0 \\ \frac{(-P+\tau_{\theta\theta})}{r_0\varrho_0 V_0} \\ 0 \\ 0 \end{bmatrix}.$$

We can then define the operators L_x as the solution of $\frac{\partial U}{\partial t} + \frac{\partial E}{\partial x} = 0$ as

$$\text{Predictor:} \qquad U_{i,j}^{\overline{**}} = U_{i,j}^* - \frac{\Delta t}{\Delta x}(E_{i+1,j}^* - E_{i,j}^*)$$

$$\text{Corrector:} \qquad U_{i,j}^{**} = \frac{1}{2}(U_{i,j}^* + U_{i,j}^{\overline{**}} - \frac{\Delta t}{\Delta x}(E_{i,j}^{\overline{**}} - E_{i-1,j}^{\overline{**}})).$$

Define the operator L_y as the solution of $\frac{\partial U}{\partial t} + \frac{\partial F}{\partial y} = 0$ as

$$\text{Predictor:} \qquad U_{i,j}^{\overline{**}} = U_{i,j}^* - \frac{\Delta t}{\Delta y}(F_{i+1,j}^* - F_{i,j}^*)$$

$$\text{Corrector:} \qquad U_{i,j}^{**} = \frac{1}{2}(U_{i,j}^* + U_{i,j}^{\overline{**}} - \frac{\Delta t}{\Delta y}(F_{i,j}^{\overline{**}} - F_{i-1,j}^{\overline{**}})).$$

Define the operator L as the solution of $\frac{\partial U}{\partial t} + H = 0$ as

$$\text{Predictor:} \qquad U_{i,j}^{\overline{**}} = U_{i,j}^* - \Delta t H_{i,j}^*$$

$$\text{Corrector:} \qquad U_{i,j}^{**} = \frac{1}{2}(U_{i,j}^* + U_{i,j}^{\overline{**}} - \Delta t H_{i,j}^{\overline{**}})$$

where $F^*_{i,j} = F(U^*_{i,j}), H^{\overline{**}}_{i,j} = H(U^{\overline{**}}_{i,j})$, etc.

The method of operator splitting requires that we time march according to the sequence of operators

$$U^{n+2}_{i,j} = L_x\, L_y\, L\, L\, L_y\, L_x\, U^n_{i,j}.$$

Factorization Schemes

The system (42) is written as

$$\frac{\Delta U}{\Delta t} + \frac{\partial}{\partial x}\left(E + \frac{\partial E}{\partial U}\Delta U\right) + \frac{\partial}{\partial y}\left(F + \frac{\partial F}{\partial U}\Delta U\right) + H + \frac{\partial H}{\partial U}\Delta U = 0 \qquad (114)$$

which can be written in the operator form

$$\left[I + \Delta t\frac{\partial}{\partial x}A\cdot + \Delta t\frac{\partial}{\partial y}B\cdot + \Delta t\, C\right]\Delta U^{n+1} = -\Delta t\,\Delta U^n_{i,j} \qquad (115)$$

where $A = \frac{\partial E}{\partial U}$, $B = \frac{\partial F}{\partial U}$, $C = \frac{\partial H}{\partial U}$ are Jacobian matrices and

$$\Delta U^n_{i,j} = \left(\frac{\partial E}{\partial x} + \frac{\partial F}{\partial y} + H\right)^n_{i,j}.$$

Here we have used the notation

$$\left(\frac{\partial}{\partial x}\cdot A\right)\Delta U^{n+1} \quad \text{to mean} \quad \frac{\partial}{\partial x.}(A\,\Delta U)$$

For example, if $\Delta = \Delta_x$ is a forward difference operator we may write

$$\frac{\partial}{\partial x}(A\Delta U) \approx \frac{\Delta_x}{\Delta x}(A\Delta U) = (A_{i+1,j}U_{i+1,j} - A_{i,j}U_{i,j})/\Delta x$$

and if $\Delta = \nabla_x$ is a backward difference operator, we would write

$$\frac{\partial}{\partial x}(A\Delta U) \approx \frac{\nabla_x}{\Delta x}(A\Delta U) = (A_{i,j}\Delta U_{i,j} - A_{i-1,j}\Delta U_{i-1,j})/\Delta x$$

with similar results applicable to the forward and backward difference operators ∇_y and Δ_y in the $y-$direction.

We desire to obtain the steady state solution to the system of equation (117). Toward this purpose, several factorization techniques have been investigated. Two such techniques are currently being used. One technique involves the predictor-corrector algorithm

Predictor:

$$\left[I + \Delta t \frac{\Delta_x}{\Delta x} A \cdot + \Delta t \frac{\Delta_y}{\Delta y} B \cdot + \Delta t\, C\right] \overline{\Delta U}_{i,j}^{n+1} = -\Delta t\, \Delta U_{i,j}^{n}$$

$$\overline{U}_{i,j}^{n+1} = U_{i,j}^{n} + \overline{\Delta U}_{i,j}^{n}$$

where Δ_x,Δ_y are forward difference operators in the x and y directions.

Corrector:

$$\left[I + \Delta t \frac{\nabla_x}{\Delta x} A \cdot + \Delta t \frac{\nabla_y}{\Delta y} B \cdot + \Delta t\, C\right] = -\overline{\Delta U}_{i,j}^{n}$$

$$U_{i,j}^{n+1} = \frac{1}{2}\left(U_{i,j}^{n} + \overline{U}_{i,j}^{n+1} + \overline{\Delta U}_{i,j}^{n+1}\right)$$

where ∇_x,∇_y are backward difference operators in the x and y directions. This algorithm gives rise to upper and lower triangular systems of equations which can be solved at each time step.

Another way to solve the system of equations (4) is to write it in the factored form

$$\left[I + \Delta t \frac{\partial A}{\partial x}\right]\left[I + \Delta t \frac{\partial B}{\partial y} + \Delta t\, C\right] \Delta U_{i,j}^{n+1} = -\Delta t\, \Delta U_{i,j}^{n}.$$

Using central differences there results tridiagonal systems of equations to solve. Both of the above methods have been programmed and are working. However, these methods, as well as the previous methods, all suffer from the CFL (Courant-Fredrich-Lewy) time step restrictions which requires that small time steps be taken in order to achieve numerical stability.

The explicit-implicit MacCormack method.

The explicit-implicit predictor-corrector algorithm given by:

Predictor with forward differencing

$$\left(\Delta U_{ij}\right)_{Explicit} = -\Delta t\left(\frac{\Delta_x E_{ij}^{n}}{\Delta x} + \frac{\Delta_y F_{ij}^{n}}{\Delta y} + H_{ij}^{n}\right) \tag{116}$$

with implicit system

$$\left(I + \Delta t \frac{\Delta_x \cdot A}{\Delta x} + \Delta t \frac{\Delta_y \cdot B}{\Delta y} + \Delta t C\right) \Delta U_{i,j}^{*n+1} = \left(\Delta U_{ij}^{n}\right)_{Explicit} \tag{116a}$$

with

$$U_{ij}^{*n+1} = U_{ij}^{n} + \Delta U_{ij}^{*n+1} \tag{116b}$$

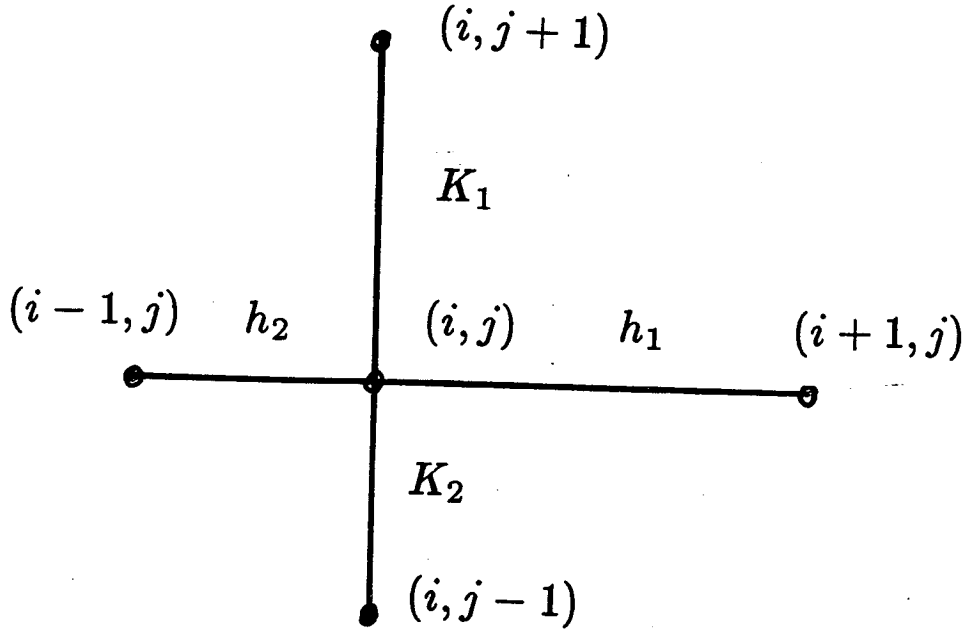

$$\frac{\partial u}{\partial x} \approx \frac{1}{h_1 + h_2}\left(\frac{h_2}{h_1}(u_{i+1,j} - u_{i,j}) + \frac{h_1}{h_2}(u_{i,j} - u_{i-1,j})\right)$$

$$\frac{\partial u}{\partial y} \approx \frac{1}{k_1 + k_2}\left(\frac{k_2}{k_1}(u_{i,j+1} - u_{i,j}) + \frac{k_1}{k_2}(u_{i,j} - u_{i,j-1})\right)$$

Figure 7. Irregular space grid points and first derivative approximations.

Corrector with backward differencing

$$\left(\overline{\Delta U_{ij}}\right)_{Explicit} = -\Delta t\left(\frac{\nabla_x (E^*)^n_{ij}}{\Delta x} + \frac{\nabla_y (F^*)^n_{ij}}{\Delta y} + (H^*)^n_{ij}\right) \tag{117}$$

with implicit system

$$\left(I + \Delta t\frac{\nabla_x \cdot A}{\Delta x} + \Delta t\frac{\nabla_y \cdot B}{\Delta y} + \Delta t C\right)\Delta U^{n+1}_{i,j} = \left(\overline{\Delta U^n_{ij}}\right)_{Explicit} \tag{117a}$$

with

$$U^{n+1}_{ij} = \frac{1}{2}\left[U^n_{ij} + (U^*)^{n+1}_{ij} + \Delta U^{n+1}_{ij}\right] \tag{117b}$$

The predictor corrector equations are applied to a rectangular i,j grid where $1 \leq i \leq ms$ and $1 \leq j \leq ns$, with boundary terms given by $i = 0, j = 0, i = msp = ms + 1, j = nsp = ns+1$. At certain i,j nodes of the grid we employ a variable grid spacing h_1, h_2, k_1, k_2 as illustrated in the figure 7 along with appropriate differencing relations. The equations (117), when expanded over the i,j grid, produces a system of equations to solve. In this system of equations there are boundary terms where along the boundary certain differences must be approximated. (reference [1]).

Steger-Warming Vector Splitting

The Steger-Warming Vector Splitting is used by Mr. J.G. Landry in his thesis to solve the nonequilibrium model 2. The method is described in his thesis. Upon completion of the thesis it will be added as an addendum to this report.

Final form of governing equations

In matrix form the basic equations are written as

$$\frac{\partial U'}{\partial t'} + \frac{1}{r^\alpha}\frac{\partial (rG')}{\partial r} + \frac{\partial F'}{\partial z} + \frac{1}{r^\alpha}H' = 0$$

where $\alpha = 0$ is for two dimensional flow and $\alpha = 1$ is for axisymmetric flow, and

$$U = \text{col}(\varrho, \varrho V_r, \varrho V_z, e_t) \tag{118}$$

and

$$G' = \begin{bmatrix} \varrho V_r \\ \varrho V_r V_r + P - \tau_{rr} \\ \varrho V_r V_z - \tau_{rz} \\ (e_t + P)V_r - V_r\tau_{rr} - V_z\tau_{rz} + q_r \end{bmatrix}$$

with

$$F' = \begin{bmatrix} \varrho V_z \\ \varrho V_r V_z + P - \tau_{rz} \\ \varrho V_z V_z + P - \tau_{zz} \\ (e_t + P)V_z - V_r\tau_{rz} - V_z\tau_{zz} + q_z \end{bmatrix} \qquad H' = \begin{bmatrix} 0 \\ -P + \tau_{\theta\theta} \\ 0 \\ 0 \end{bmatrix}.$$

We introduce the nondimensional variables

$$r^* = \frac{r}{L}, \quad z^* = \frac{z}{L}, \quad V_r^* = \frac{V_r}{V_0}, \quad V_z = \frac{V_z}{V_0}, \quad \rho^* = \frac{\rho}{\rho_0}$$
$$t^* = \frac{t}{L/V_0}, \quad \eta^* = \frac{\eta}{\eta_0}, \quad P^* = \frac{P}{\rho_0 V_0^2}, \quad T^* = \frac{T}{T_0}, \quad e^* = \frac{e}{V_0^2}$$

then the above equations become

$$\frac{\partial U^*}{\partial t^*} + \frac{1}{r^{*\alpha}}\frac{\partial}{\partial r^*}(r^* G^*) + \frac{\partial F^*}{\partial z^*} + \frac{1}{r^*}H^* = 0,$$

with

$$U^* = \begin{bmatrix} \rho^* \\ \rho^* V_r^* \\ \rho^* V_z^* \\ e_t^* \end{bmatrix}, \qquad G^* = \begin{bmatrix} \rho^* V_r^* \\ \rho^* V_r^{*2} + P^* - \frac{1}{Re}\tau_{rr}^* \\ \rho^* V_r^* V_z^* - \frac{1}{Re}\tau_{rz}^* \\ (e_t^* + P^*)V_r^* - \frac{1}{Re}V_r^*\tau_{rr}^* - \frac{1}{Re}V_z^*\tau_{rz} + q_r^* \end{bmatrix}$$

and

$$F^* = \begin{bmatrix} \rho^* V_z^* \\ \rho^* V_r^* V_z^* - \frac{1}{Re}\tau_{rz}^* \\ \rho^* V_z^{*2} + P^* - \frac{1}{Re}\tau_{zz}^* \\ (e_t^* + P^*)V_z^* - \frac{1}{Re}V_r^*\tau_{rz}^* - \frac{1}{Re}V_z^*\tau_{zz}^* + q_z^* \end{bmatrix}, \qquad H^* = \begin{bmatrix} 0 \\ -P^* + \frac{1}{Re}\tau_{\theta\theta}^* \\ 0 \\ 0 \end{bmatrix}$$

where

$$e_t^* = \rho^* e^* + \frac{\rho^*}{2}(V_r^{*2} + V_z^{*2})$$

$$\tau_{zz}^* = 2\eta^* \frac{\partial V_z^*}{\partial x^*} + \lambda^* \left(\frac{1}{r^*}\frac{\partial}{\partial r^*}(r^* V_r^*) + \frac{\partial v_z^*}{\partial x^*} \right)$$

$$\tau_{rz}^* = \eta^* \left(\frac{\partial V_z^*}{\partial r^*} + \frac{\partial V_r^*}{\partial z^*} \right)$$

$$\tau_{rr}^* = 2\eta^* \frac{\partial V_r^*}{\partial r^*} + \lambda^* \left(\frac{1}{r^*}\frac{\partial}{\partial r^*}(r^* V_r^*) + \frac{\partial v_z^*}{\partial x^*} \right)$$

$$\tau_{\theta\theta}^* = 2\eta^* \frac{V_r^*}{r^*} + \lambda^* \left(\frac{1}{r^*}\frac{\partial}{\partial r^*}(r^* V_r^*) + \frac{\partial v_z^*}{\partial x^*} \right)$$

$$\tau_{zz}^* = 2\eta^* \frac{\partial V_z^*}{\partial z^*} + \lambda^* \left(\frac{1}{r^*}\frac{\partial}{\partial r^*}(r^* V_r^*) + \frac{\partial v_z^*}{\partial x^*} \right)$$

and

$$Re = \frac{\rho_0 V_0 L}{\eta_0}, \quad e_t = e_{t0} e_t^*, \quad e_{t0} = \rho_0 V_0^2, \quad \lambda = \eta_0 \lambda^*.$$

The shape of the nozzle is given by $r = f(z)$ which becomes $r^* = f(bz^*)/b$ in the $*$ coordinates. Making the change of variable

$$x = z^*, \qquad y = \frac{r^*}{f(bz^*)/b},$$

the final form of the equations are given by

$$\frac{\partial U^*}{\partial t^*} + \frac{\partial}{\partial y}\left(\frac{b}{f}G^* - \frac{b\,y\,f'}{f}F^*\right) + \frac{\partial F^*}{\partial x} + \frac{b}{yf}(H^* + G^*) + \frac{bf'}{f}F^* = 0.$$

In the limit as $y \to 0$ we find that

$$\lim_{y\to 0} \frac{H^* + G^*}{yf} = \frac{b}{f} \begin{bmatrix} \rho^* \frac{\partial V_r^*}{\partial y} \\ 0 \\ \rho^* V_z^* \frac{\partial V_r}{\partial y} - \frac{1}{Re}\frac{\partial \tau_{rx}^*}{\partial y} \\ (e_t^* + P^*)\frac{\partial V_r^*}{\partial y} - \frac{\tau_{rr}^*}{Re}\frac{\partial V_r^*}{\partial y} - \frac{1}{Re}\left(V_z^* \frac{\partial \tau_{rx}^*}{\partial y} + \tau_{rz}\frac{\partial V_x^*}{\partial y}\right) + \frac{\partial q_r^*}{\partial y} \end{bmatrix}.$$

The above equations are to be solved over the computational domain $0 \le z^* \le 1$ and $0 \le r \le f(z)$ where $f(z)$ defines the shape of the nozzle.

SUMMARY MODEL 1 (EQUILIBRIUM THERMODYNAMICS)

Continuity Equation

$$\frac{D\rho}{Dt} + \rho\nabla \cdot \vec{V} = 0$$

Equation of State

$$P = \rho RT$$

Momentum Equation

$\rho\frac{D\vec{V}}{Dt} = -\nabla \cdot \mathbf{P}$ where $P_{ij} = P\delta_{ij} - \eta(v_{i,j} + v_{j,i} - \frac{2}{3}\delta_{ik}v_{k,k})$ and η is given by the Sutherland formula

$$\eta = \frac{c_1 g_c T^{3/2}}{T + c_2} \quad [Kg/m\,s]$$

where for N_2 we have $c_1 = 2.16(10^{-8}) * 1.488$,$c_2 = 184.0$ and $g_c = 32.174$.

Energy Equation

$$\rho\frac{D(C_v T)}{Dt} = -[\mathbf{P} : D + \nabla \cdot \vec{q} - q_{rad}]$$

where

$$\vec{q} = -\bar{\lambda}_k \nabla T$$

$$D_{ij} = \frac{1}{2}(v_{i,j} + v_{j,i})$$

$$q_{rad} = \nabla\left(\lambda_R \nabla(\frac{4}{3}\sigma_{SB}T^4)\right)$$

SUMMARY MODEL 2 (NONEQUILIBRIUM THERMODYNAMICS)

Continuity Equation

$$\frac{D\rho}{Dt} + \rho\nabla\cdot\vec{V} = 0$$

Equation of State

$$P = \rho RT$$

Momentum Equation

$\rho\frac{D\vec{V}}{Dt} = -\nabla\cdot\mathbf{P}$ where $P_{ij} = P\delta_{ij} - \eta(v_{i,j} + v_{j,i} - \frac{2}{3}\delta_{ik}v_{k,k})$ and η is given by the Sutherland formula

$$\eta = \frac{c_1 g_c T^{3/2}}{T + c_2} \quad [Kg/m\,s]$$

where for N_2 we have $c_1 = 2.16(10^{-8}) * 1.488$,$c_2 = 184.0$ and $g_c = 32.174$.

Energy Equation

$$\rho\frac{D(C_vT)}{Dt} = -\left[\mathbf{P} : D + \nabla\cdot\vec{q}_{rt} - q_{rad} + \rho C_{vv}X\right]$$

$$\frac{DT_v}{Dt} = -\frac{\nabla\cdot\vec{q}_v}{\rho C_{vv}} + X$$

$$X = \frac{T_v^2}{\phi\tau}\left[\frac{1 - e^{-\phi/T_v}}{1 - e^{-\phi/T}}\right]\left\{\exp[\phi(\frac{1}{T_v} - \frac{1}{T}) - 1]\right\}$$

$$\phi = \frac{h\nu}{k}$$

$$C_{vv} = k\left(\frac{\phi}{T_v}\right)^2 \exp(\frac{\phi}{T_v})\left(\exp(\frac{\phi}{T_v}) - 1\right)^{-2}$$

$$\vec{q}_v = -\lambda_v\nabla T_v$$

$$\lambda_v = \eta C_{vv}/m$$

$$\vec{q}_{rt} = -\lambda_k\nabla T$$

$$\lambda_k = 19\eta k/4m$$

$$\tau_{mw} = \frac{1}{p(atm)}\exp\{A(T^{-1/3} - 0.015\mu^{1/4}) - 18.42\}$$

$$\tau = \left(\frac{T}{5000}\right)^{3/2}\left[\frac{1 - \exp(-\phi/5000)}{1 - \exp(-\phi/T)}\right]\tau_{mw}$$

$$A = 220, \quad \phi = 3395, \quad \mu = 14.$$

and

$$D_{ij} = \frac{1}{2}(v_{i,j} + v_{j,i})$$

$$q_{rad} = \nabla\left(\lambda_R\nabla(\frac{4}{3}\sigma_{SB}T^4)\right)$$

Preliminary Considerations

The Knudsen number, reference [31], is defined $K_n = \lambda/d$, and is the ratio of the mean free path λ to some typical dimension in the flow field. The Navier-Stokes equations, for the simulation of gas flows, is valid when the Knudsen number is very small in comparison with unity. As the Knudsen number increases the intermolecular collisions of the gas particles becomes less. A knudsen number of 0.1 has been used, reference [29], to describe the boundary between continuum and transition regime flows. This assumption is based upon the selection of an appropriate scale length d used to determine the Knudsen number.

For internal flows, gas properties which depend upon molecular collisions such as viscosity, heat conduction, diffusion, heat capacity, etc., will be greatly altered when the Knudsen number is large. This is because molecules will collide more readily with the wall boundaries than with each other. As the density of the gas decreases, the collision rate of the molecules diminishes and eventually the continuum theory breaks down. Under such conditions one can resort to direct simulation Monte Carlo techniques associated with Boltzmann equation, as opposed to the Navier-Stokes equations, which treats the rarefied gas as a set of discrete molecules.

The maximum mean free path for N_2 is given approximately by

$$\lambda_{max}\,(cm) \approx \frac{1}{n\pi\sigma^2}$$

reference [26], where $\sigma^2 = 14.9\,(10)^{-16}\,\mathrm{cm}^2$ and n is the gas density in $molecules/cm^3$. The figure 8 illustrates the maximum mean free path vs density of Nitrogen. Using the local nozzle minimum radius as representative of d, and using the density from a one dimensional nozzle analysis, the figures 9,10,11 illustrate approximate Knudsen numbers vs distance along the nozzle. These figures illustrate that for high expansion nozzles, large pressures are required to insure the Navier-Stokes modeling remains valid.

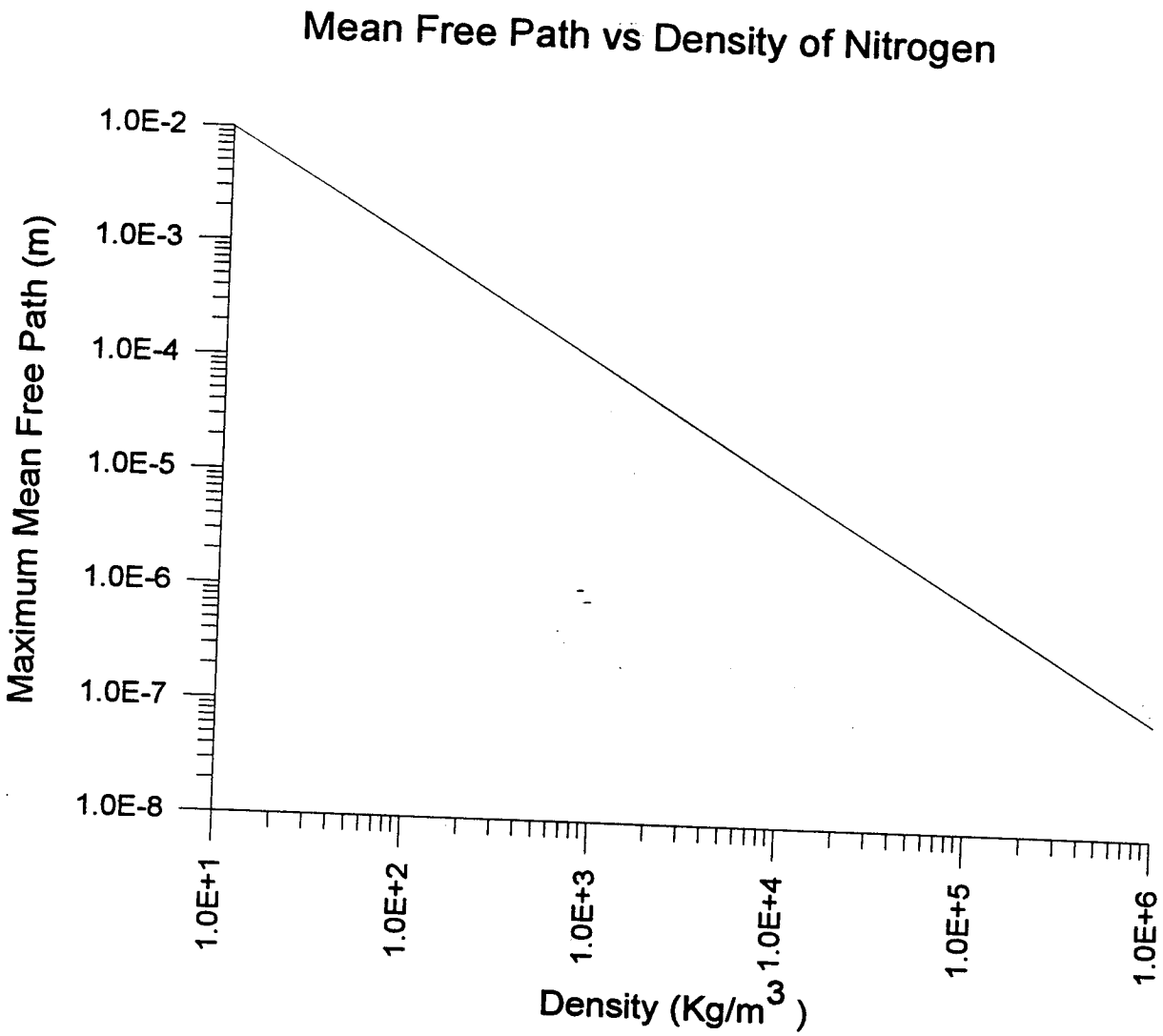

Figure 8. Mean free path vs density of Nitrogen.

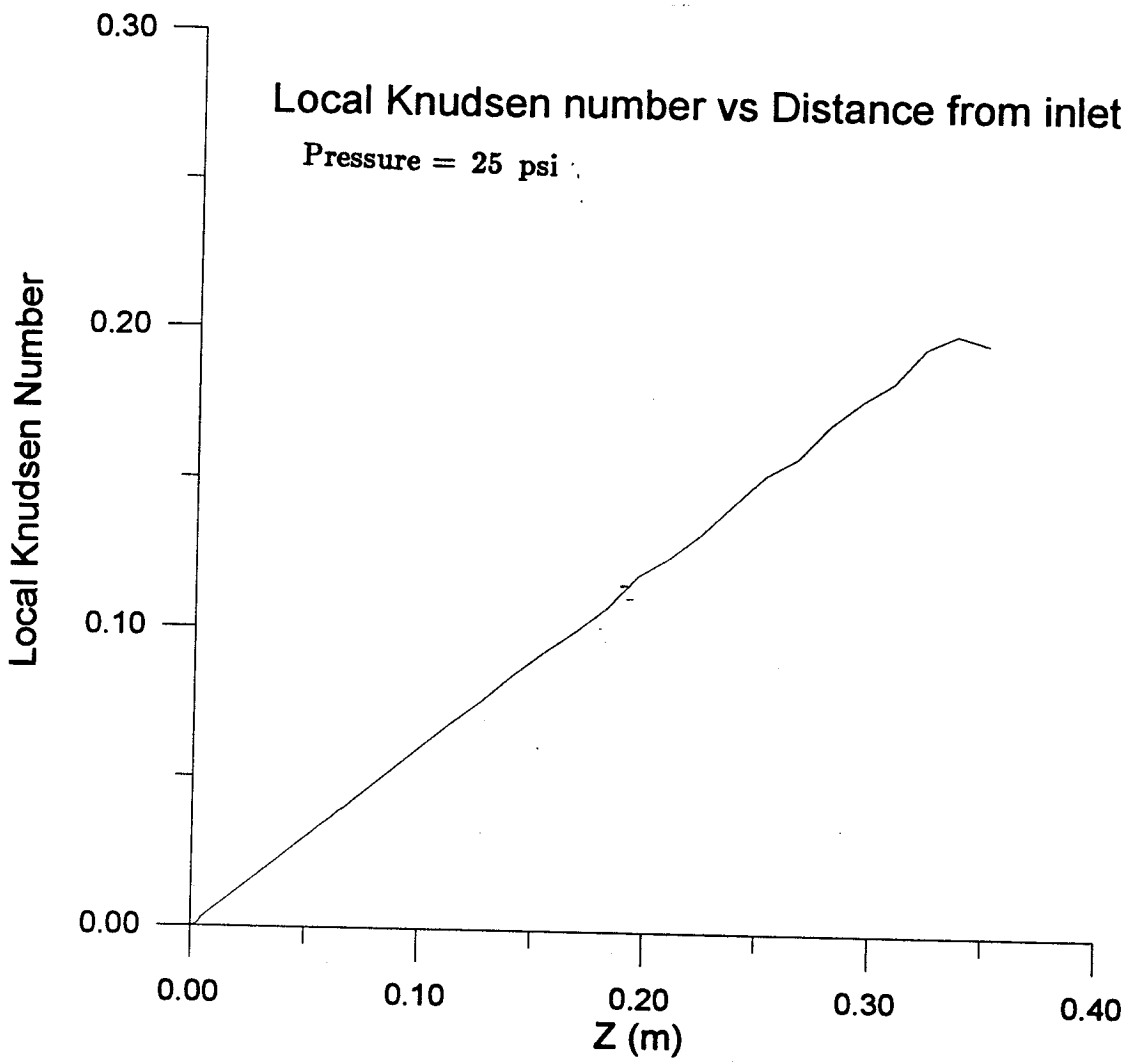

Figure 9. Knudsen number vs nozzle distance.

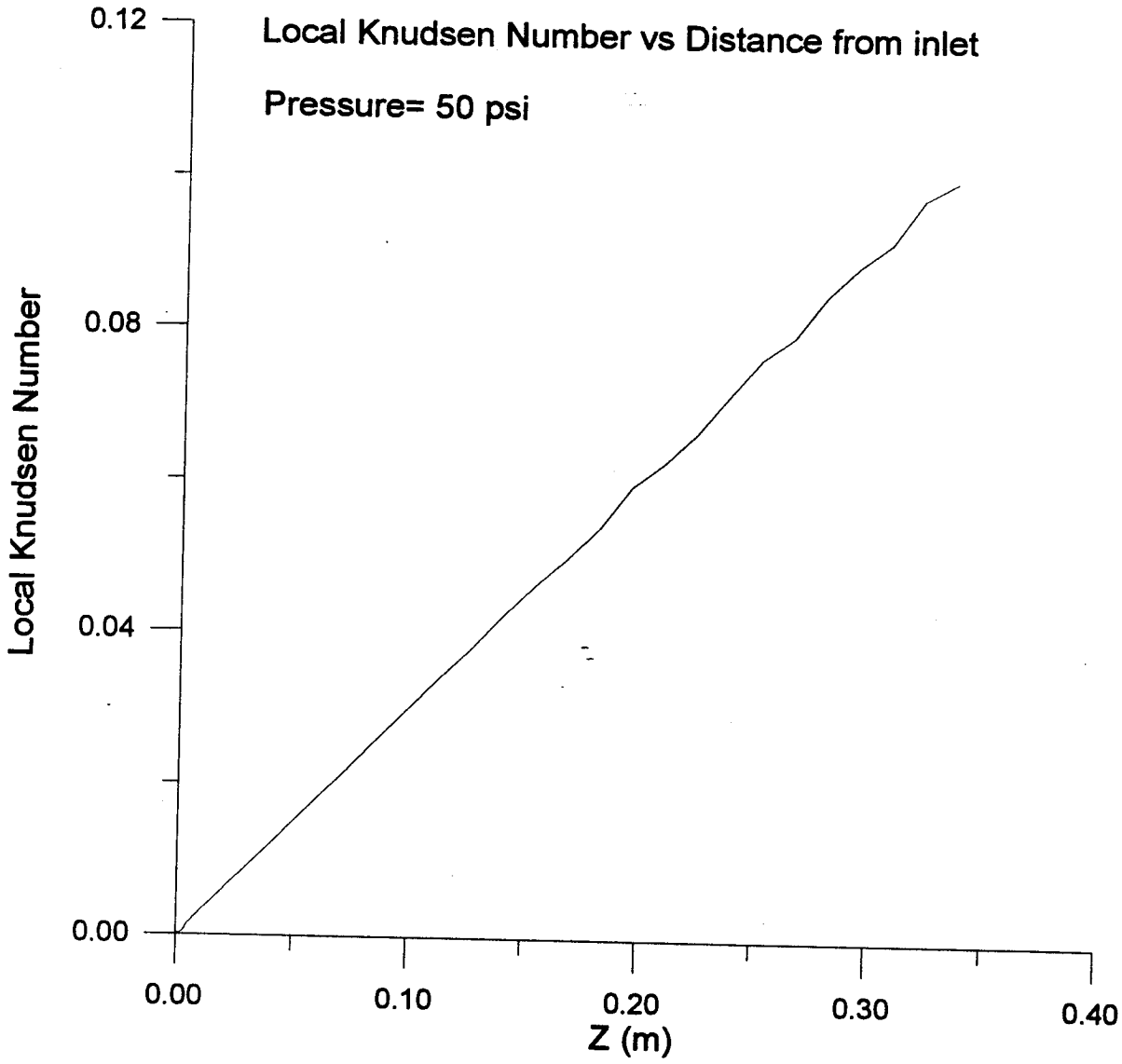

Figure 10. Knudsen number vs nozzle distance.

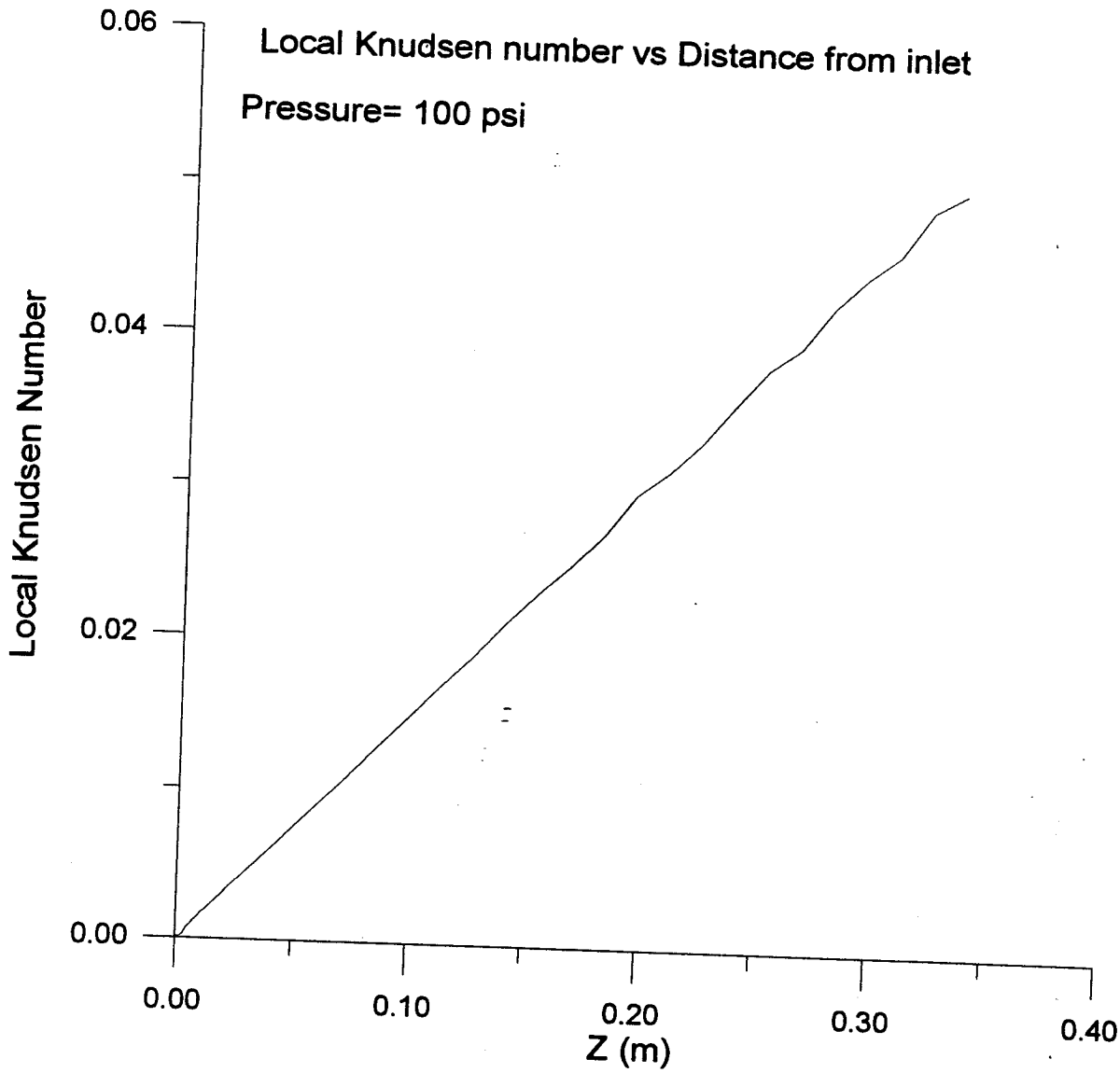

Figure 11. Knudsen number vs nozzle distance.

Conclusions

The reference [1] points out several difficulties associated with the numerical solution of the compressible Navier-Stokes equations. These difficulties are:

(i) The Courant-Friedrich-Lewy (CFL) condition for numerical stability limits the time step that the solution can be advanced.

(ii) The treatment of steep flow gradients and mesh size needed to handle these gradients.

(iii) The treatment of turbulence and associated mesh size.

(iv) Approximate factorization error in the numerical solution.

(v) Linearization error.

The figure 2 illustrates the mesh selected for the numerical solution in order to address the concerns of (ii) and (iii) above. The size of the mesh was selected to address the concerns of items (iv) and (v) above. The step size limit continued to be a problem in our numerical techniques for a solution.

The diffusion fluxes, described by the vectors E, F and H of equations (42)(43), are found from the Navier-Stokes diffusion of momentum and Fourier's heat conduction law. The viscous terms and heat conductivity, in these terms, are all temperature dependent. The heat capacity of the gas is taken from reference [19]. We also employ the Stokes hypothesis that the second coefficient of viscosity is given by $\lambda = -2\eta/3$. The exit pressure is such that a shockless supersonic flow is sustained in the diverging portion of the nozzle.

The reference [17] points out that there are no proper initial and boundary conditions that will insure existence and uniqueness of the solution. For this problem we tried to select boundary conditions that were physically realizable. we use adiabatic boundary conditions for the temperature T and required that the normal derivative of the pressure be zero at the walls. The exit values on the boundary were all extrapolated. The inlet boundary conditions were such that all values were fixed except for one variable conditions which was extrapolated (reference [27]). We investigated two different input conditions. One the extrapolation on density and the other investigated the extrapolation of velocity. The density extrapolation seemed to keep the mass flow, (continuity equation), in balance.

For model 1 we employed the explicit-implicit MacCormack method. For the model 2, the Steger-Warming technique was employed. The numerical results for the model 1 are summarized in the figures 12 through 19. The figures 12,13 illustrate the resulting temperature contours throughout the nozzle. Note the sudden drop in temperature as the gas passes through the throat. The figures 14,15 illustrate the contour plots of the

resulting radial velocity V_r, while figures 16,17 illustrate the contour plots of the axial velocity V_z. The figures 18,19 illustrate the contour plots of the logarithm of density. All nozzle dimensions are given in the appendix B.

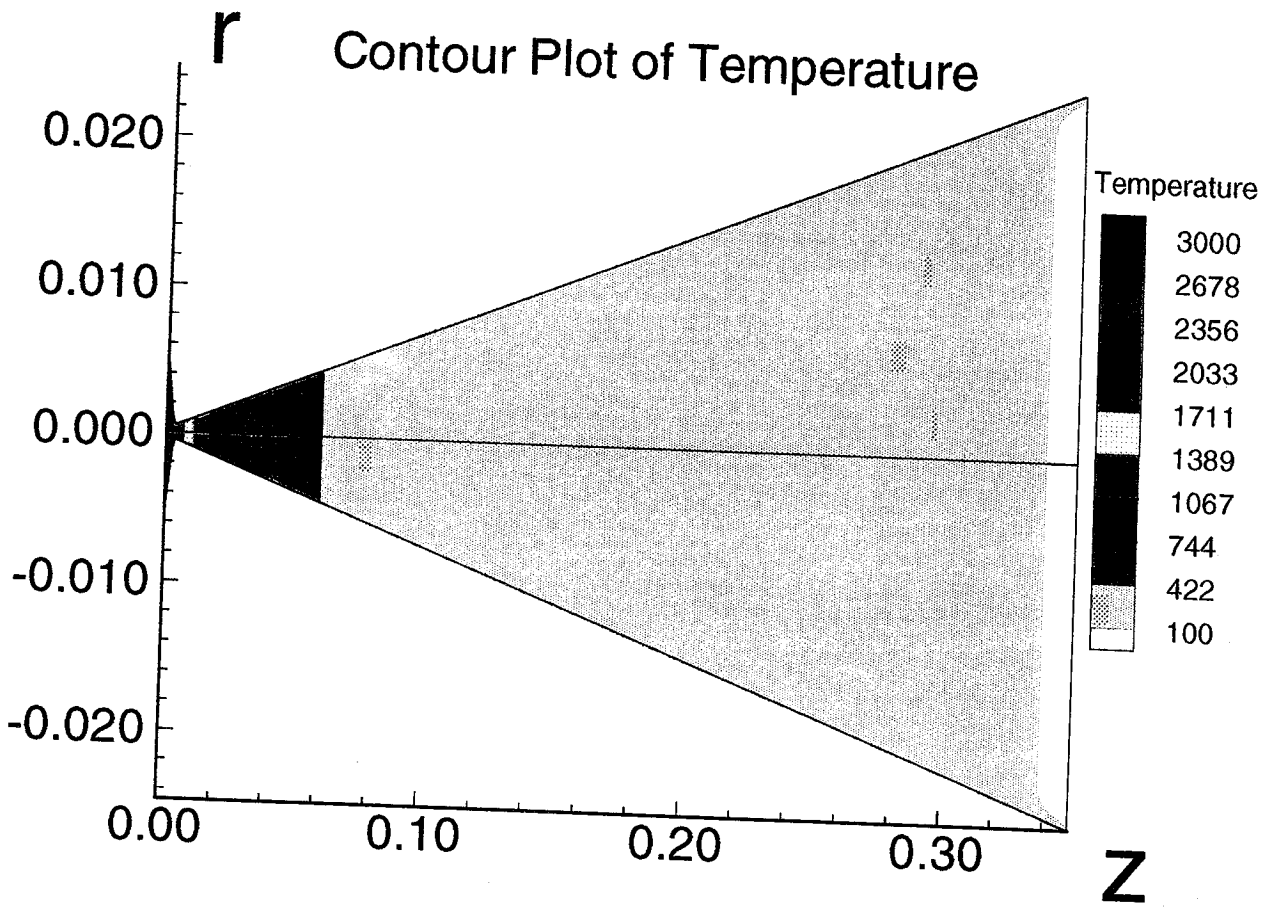

Figure 12. Contour plot of temperature.

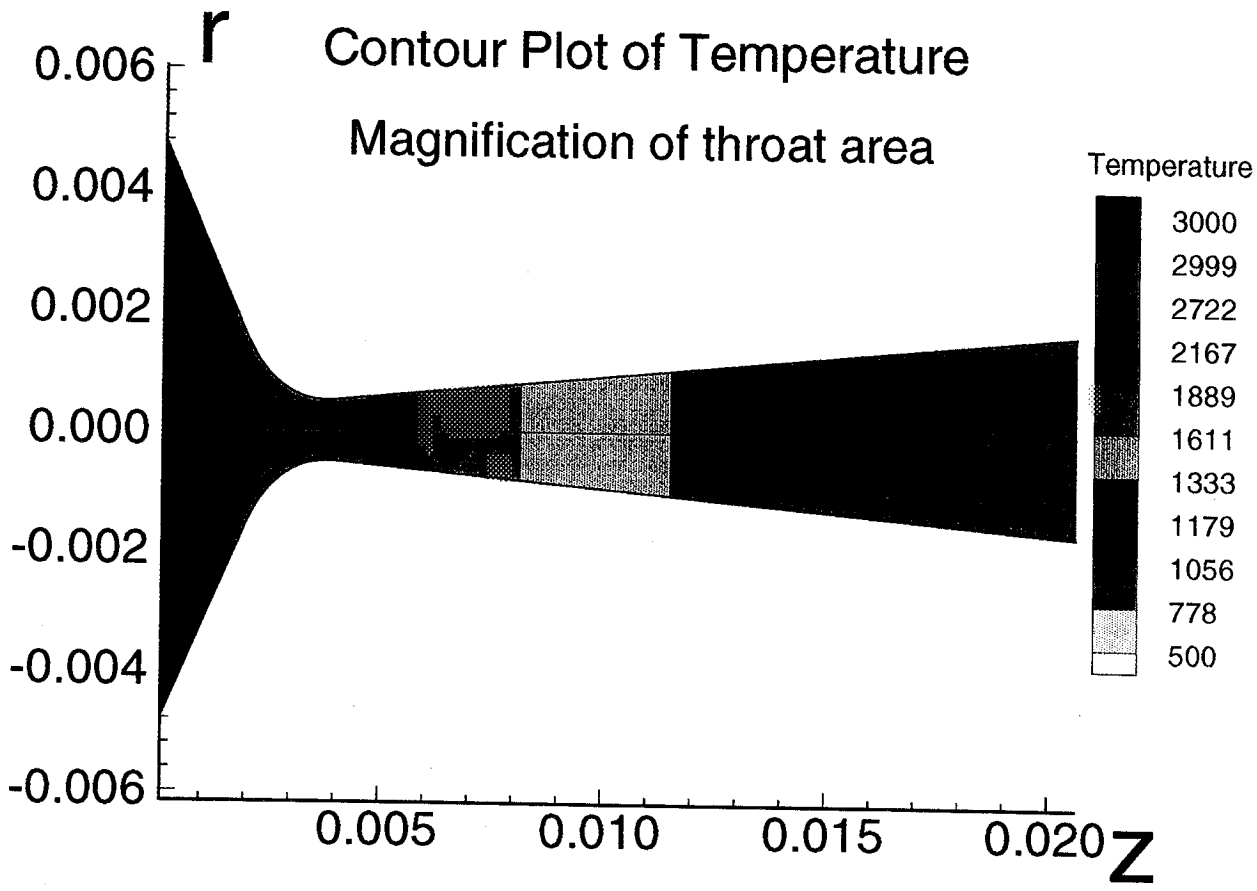

Figure 13. Contour plot of temperature.

ORIGINAL PAGE
COLOR PHOTOGRAPH

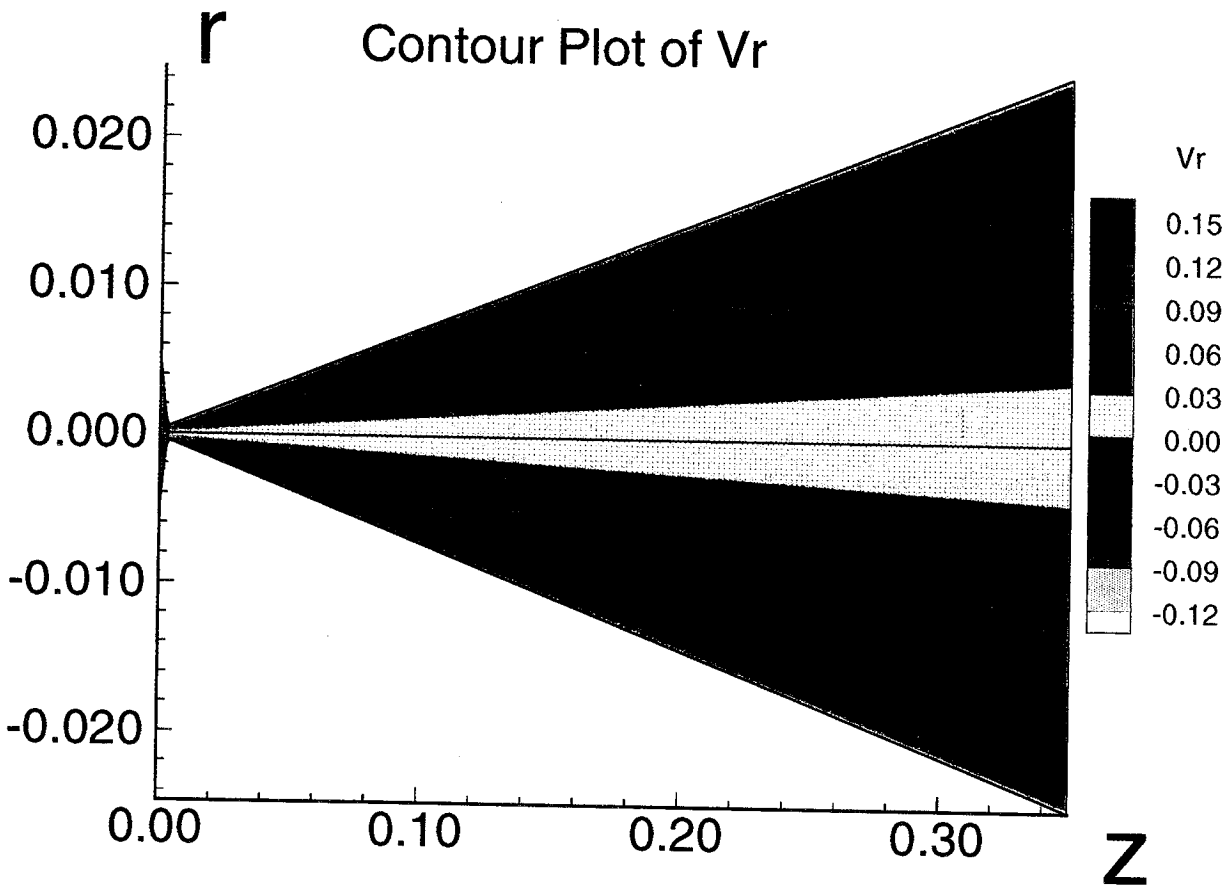

Figure 14. Contour plot of radial velocity.

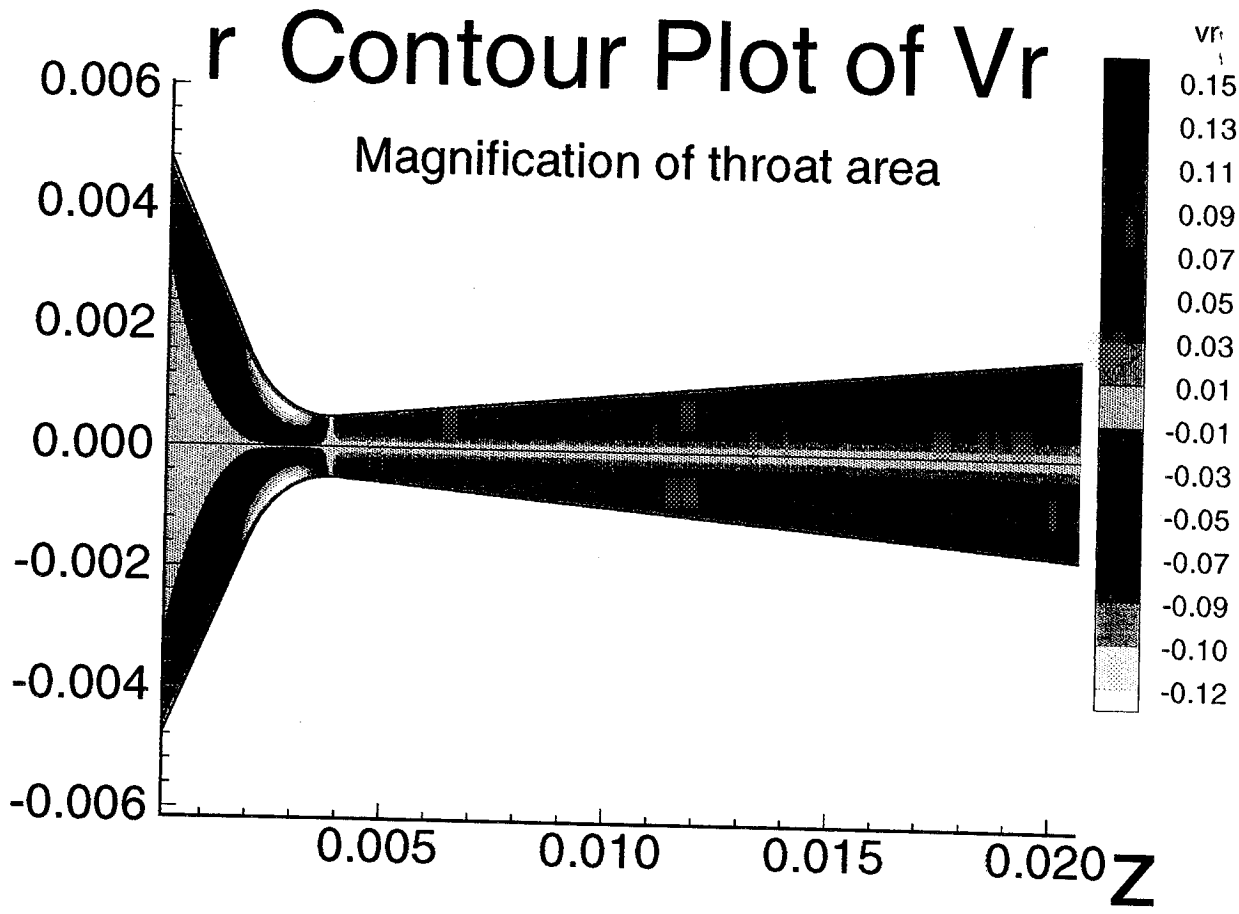

Figure 15. Contour plot of radial velocity.

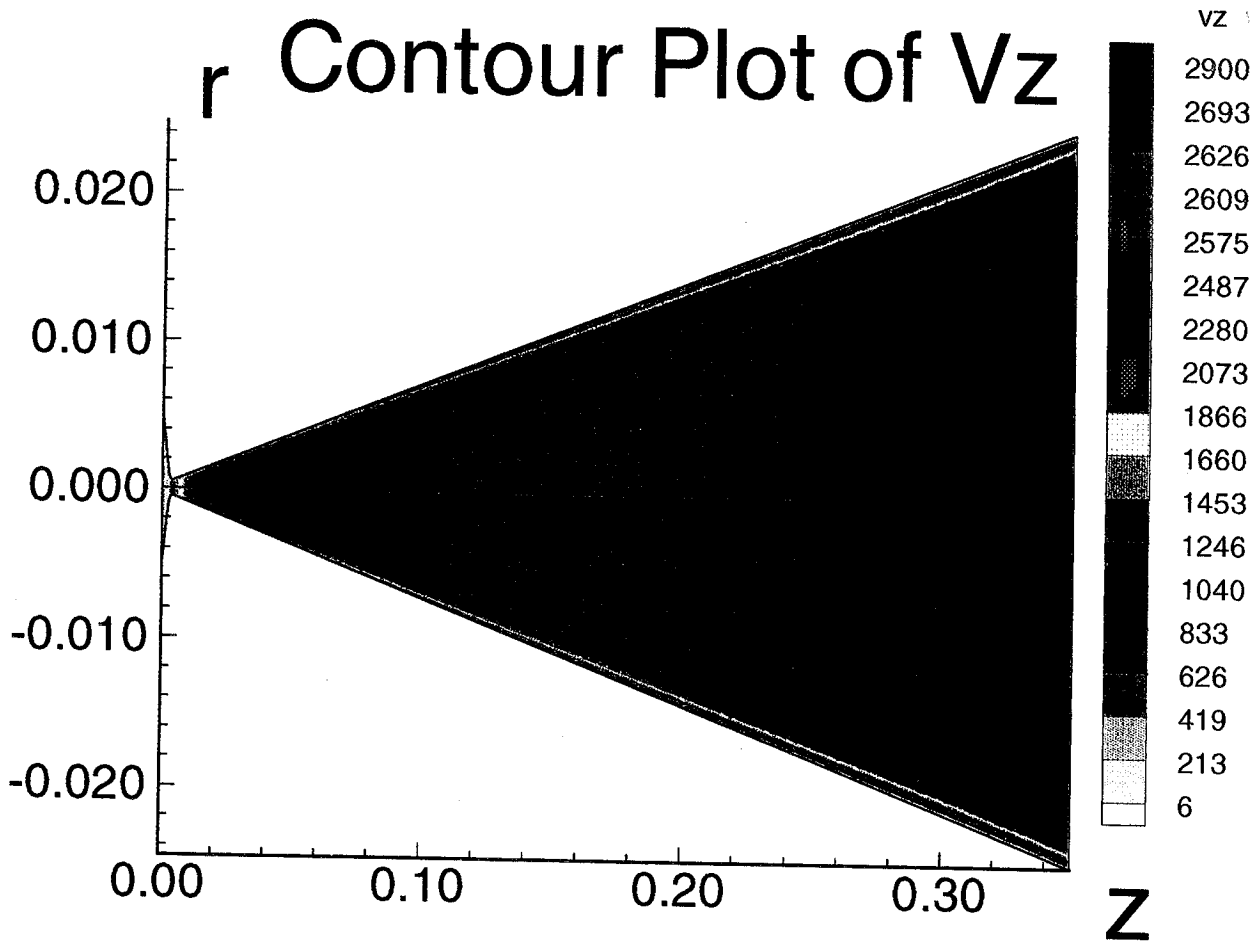

Figure 16. Contour plot of axial velocity.

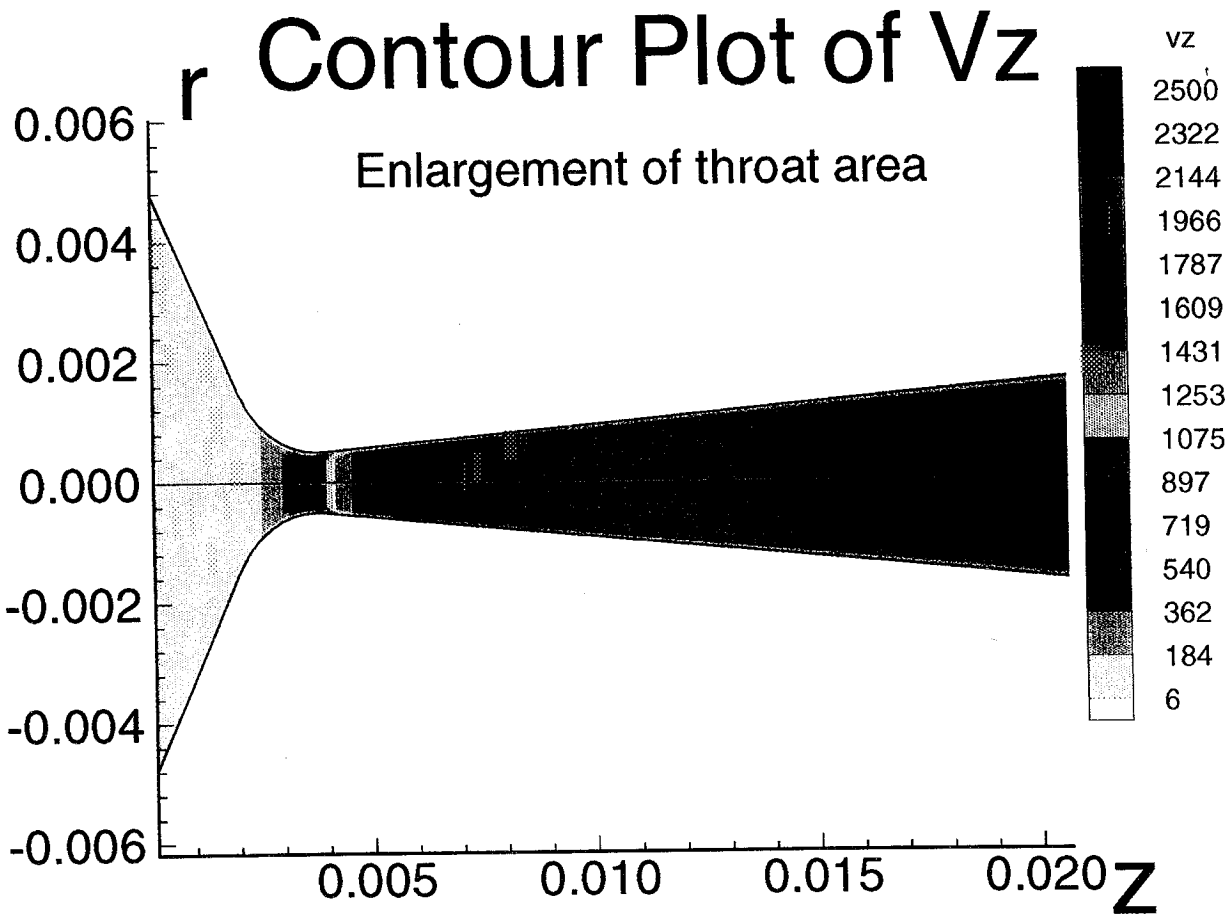

Figure 17. Contour plot of axial velocity.

ORIGINAL PAGE
COLOR PHOTOGRAPH

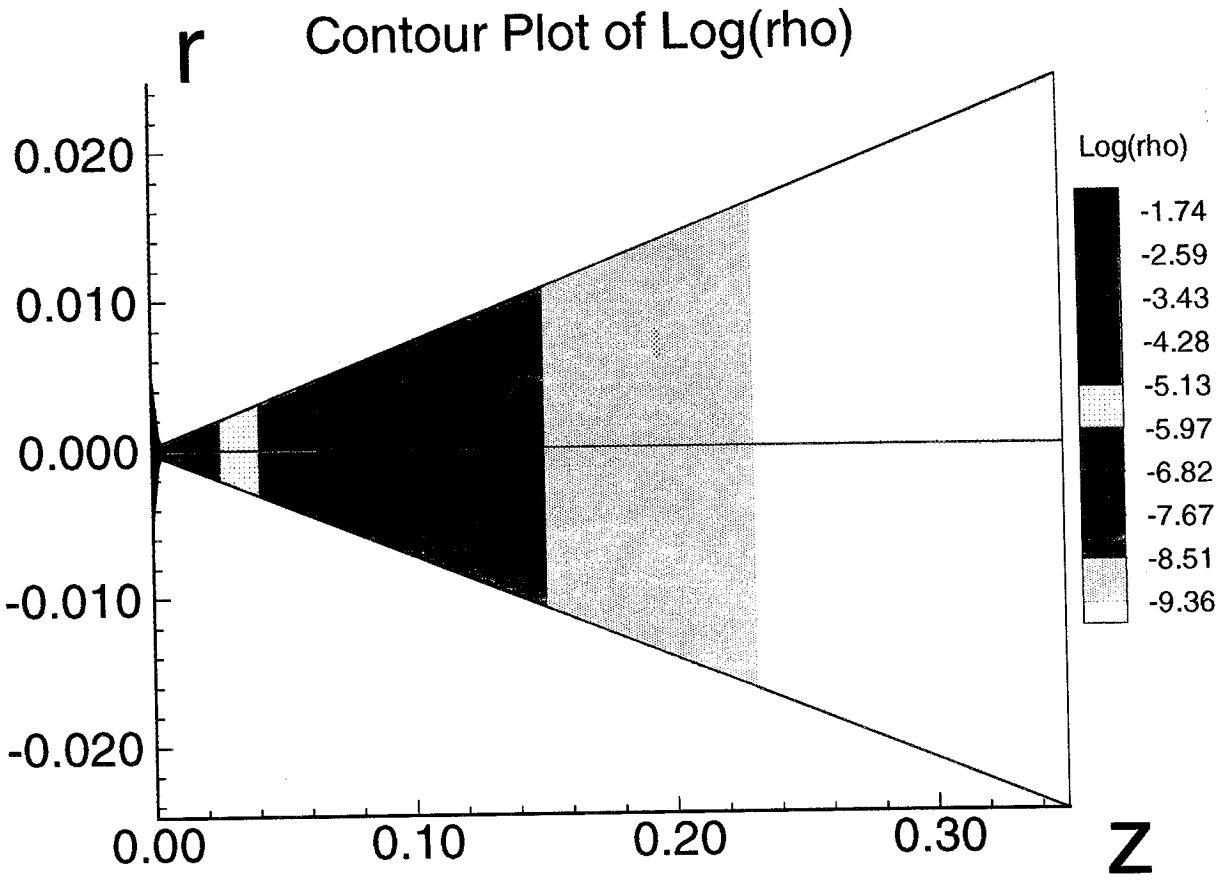

Figure 18. Contour plot of logarithm of density.

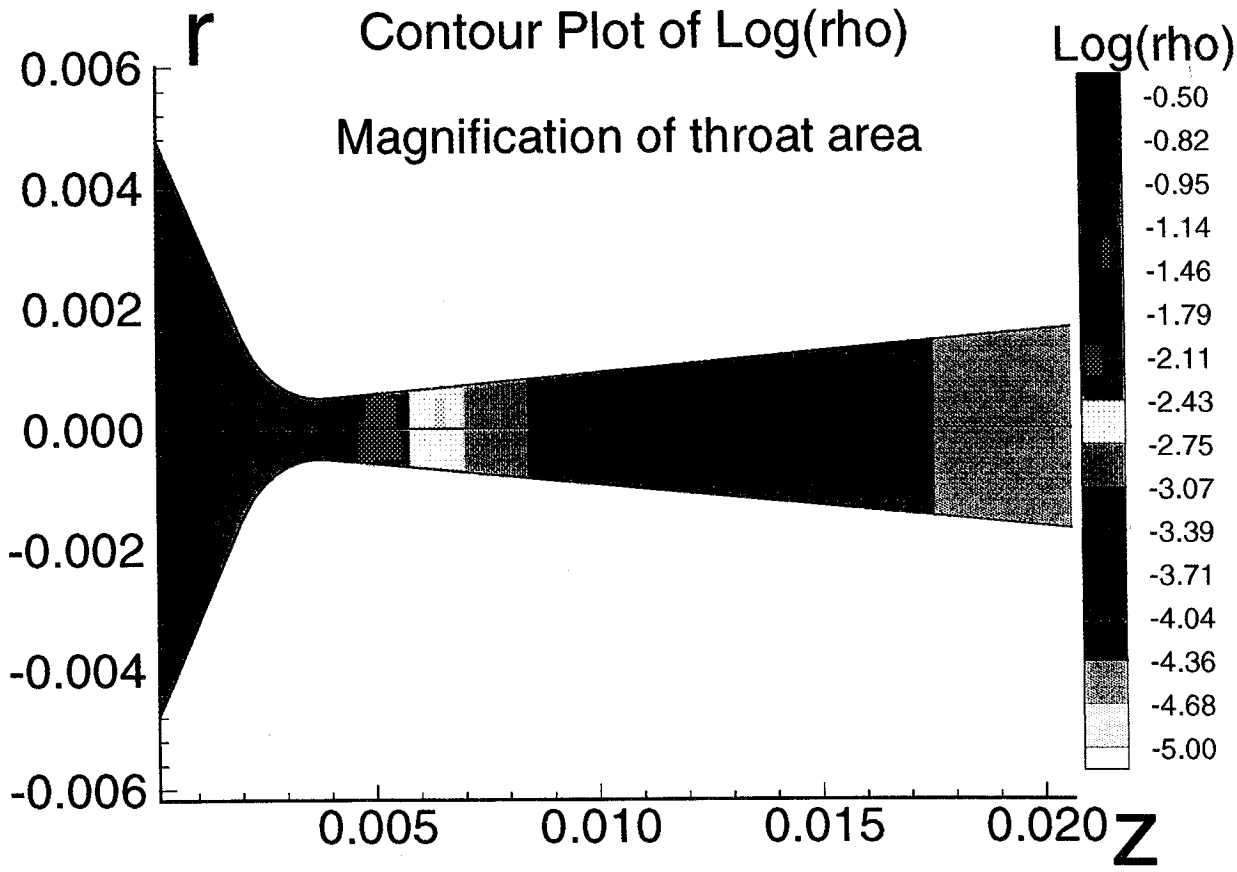

Figure 19. Contour plot of logarithm of density.

ORIGINAL PAGE
COLOR PHOTOGRAPH

The model 2 assumes nonequilibrium thermodynamics. The vibrational potential of the molecules are represented by a harmonic oscillator model, references [21],[28]. The nonequilibrium thermodynamic model is formulated with two temperatures and differs from the models developed in the references [2] and [3]. The main differences are (i) thermochemical vs thermodynamic nonequilibrium. (ii) boundary conditions. (isothermal vs adiabatic.) (iii) nozzle shape, scaling and mesh size. (iv) The representation of relaxation time over the solution domain.

The nonequilibrium model is developed from first principles. It is a two temperature model used to study thermodynamic nonequilibrium where vibrational excitation and rotational-translational excitation are the dominant nonequilibrium phenomena. Such situations arise in the study of re-entry flow and certain converging-diverging nozzle flows, reference [2]. Almost everything in model 2 is the same as in model 1 with the exception of energy and temperature representation. The vibrational relaxation follows the work of Meador, et. al., reference [7], for Nitrogen gas through a nozzle.

The numerical results for model 2 are summarized in the figures 20 through 29. The figures 20,21 are contour plots of temperature. The figures 22,23 are contour plots of vibrational temperature. The figures 24,25 are contour plots of radial velocity V_r. The figures 26,27 are contour plots of the axial velocity V_z. The figures 28,29 are contour plots of logarithm of density.

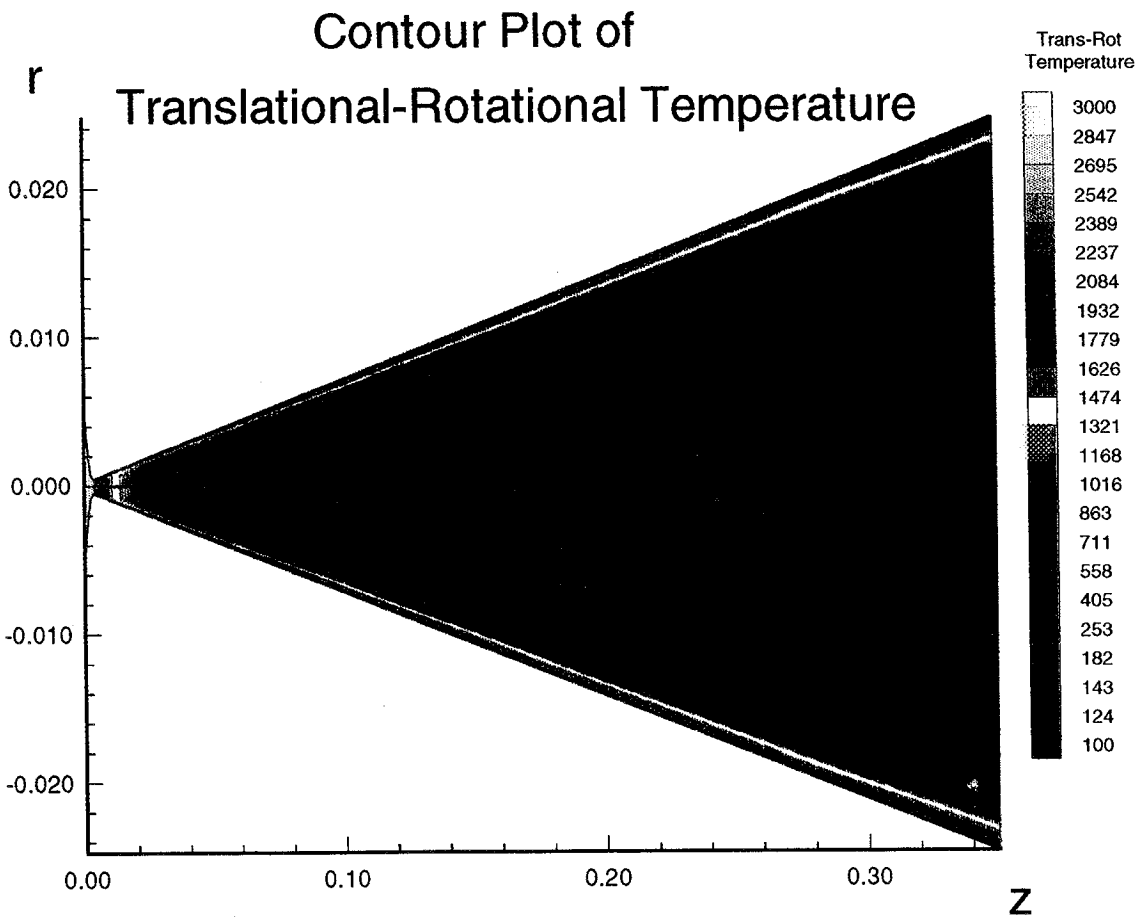

Figure 20. Contour plot of rotational-translational temperature.

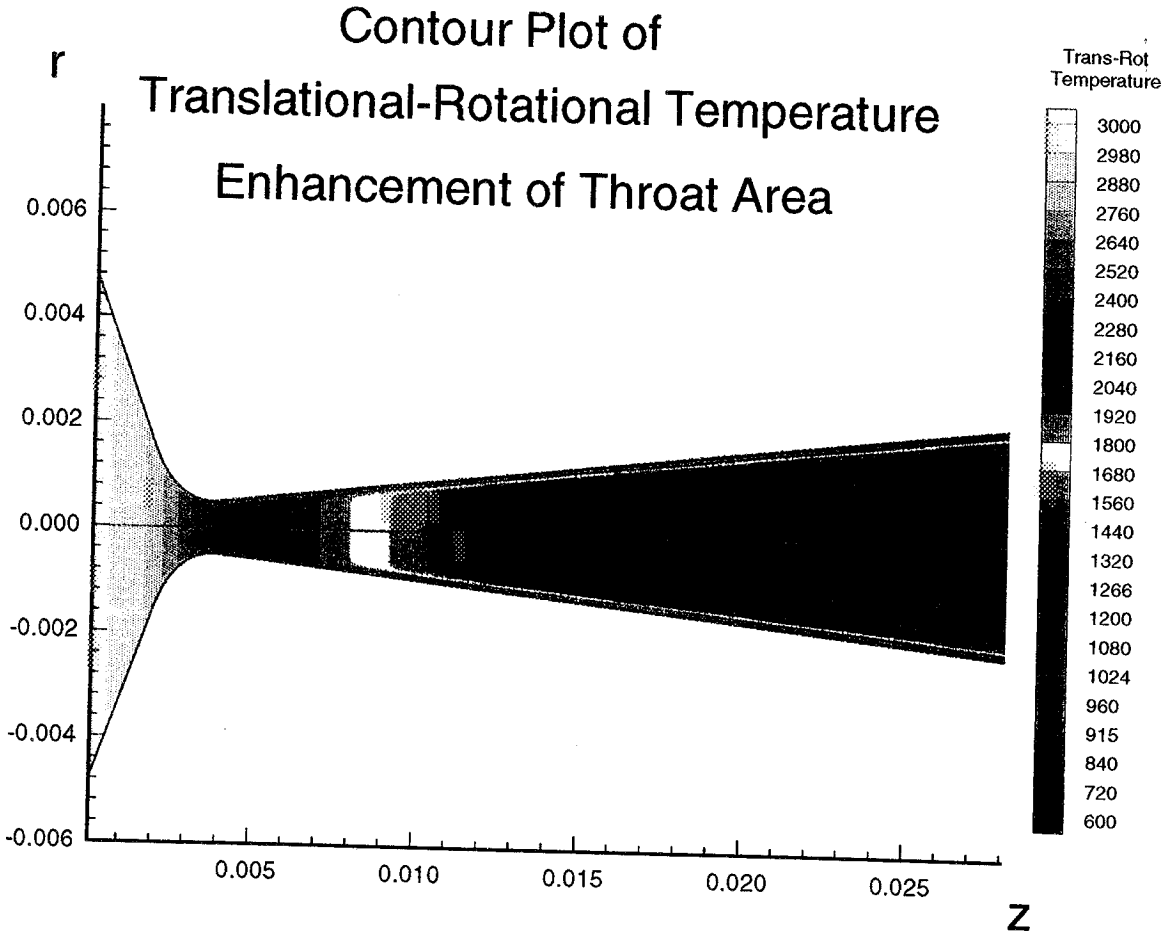

Figure 21. Contour plot of rotational-translational temperature.

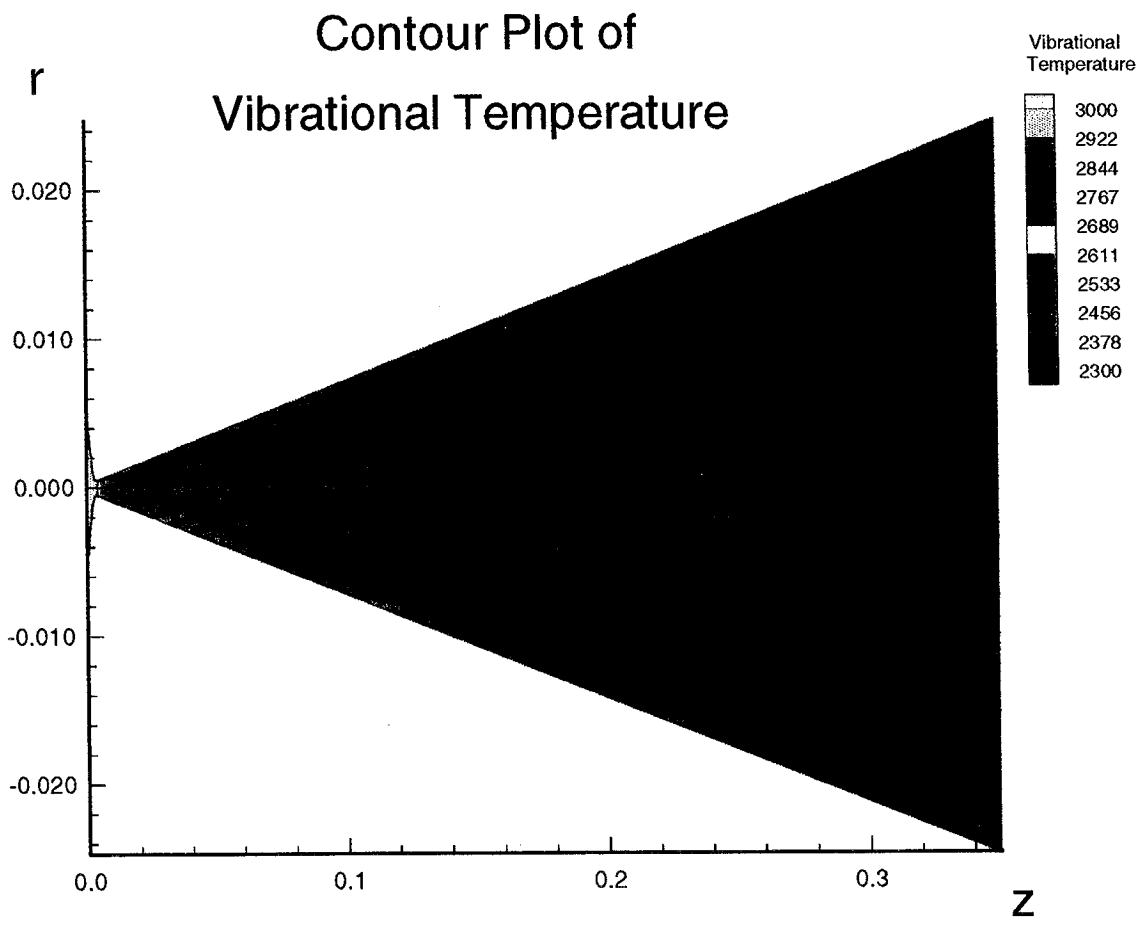

Figure 22. Contour plot of vibrational temperature.

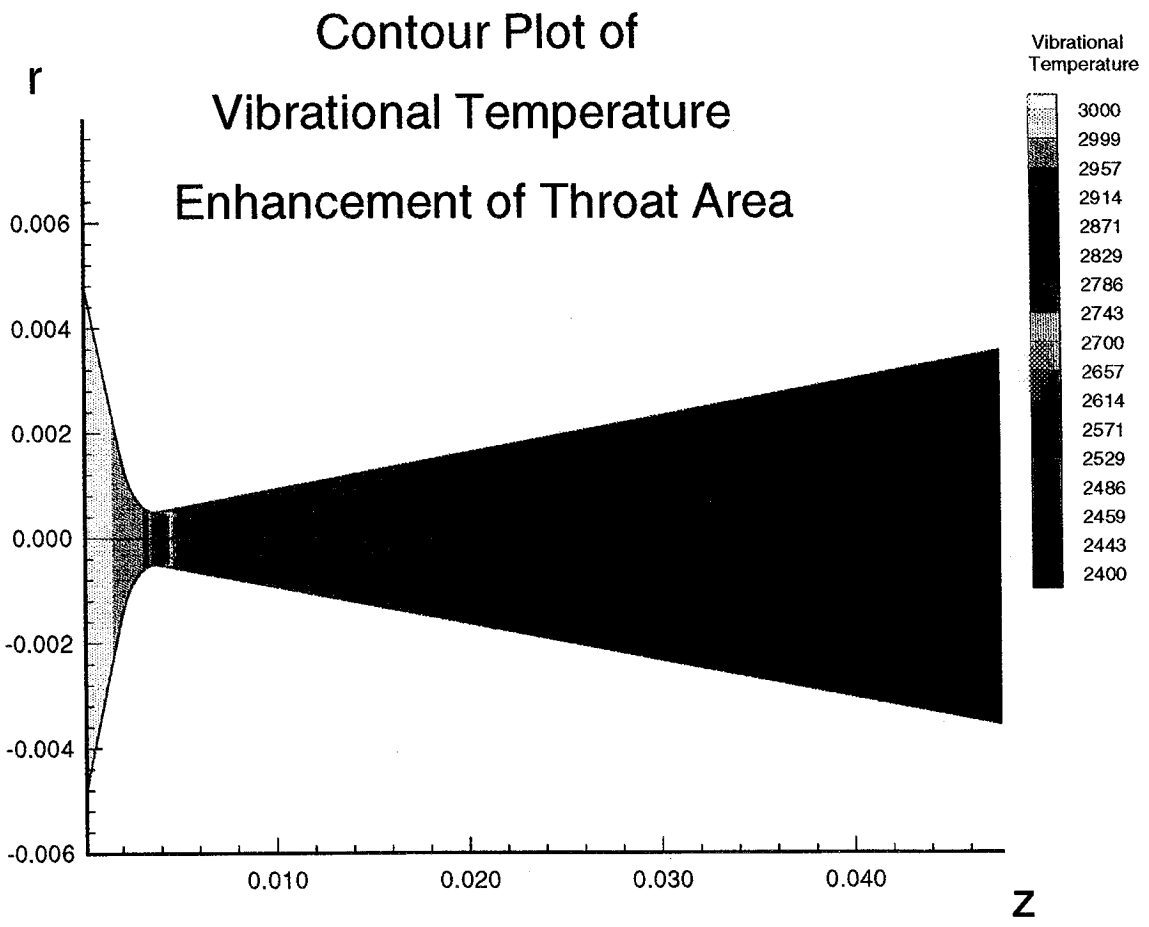

Figure 23. Contour plot of vibrational temperature.

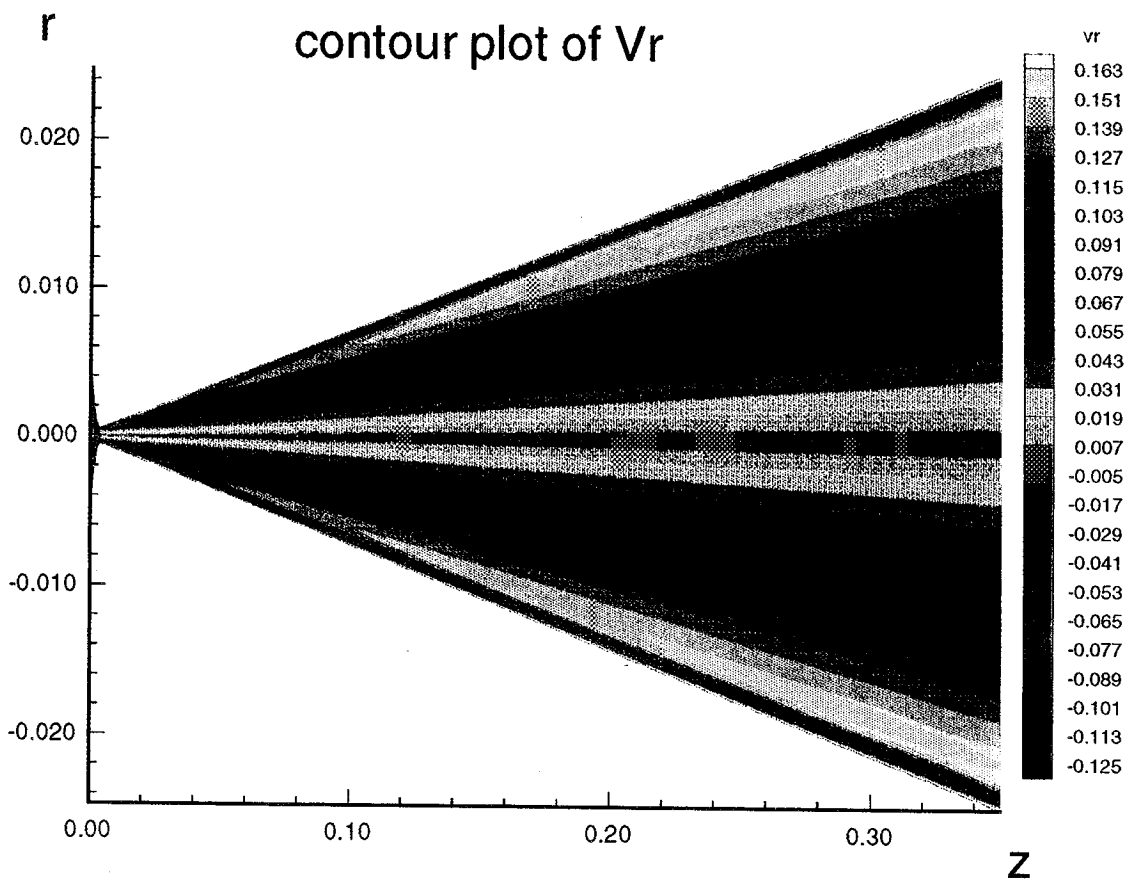

Figure 24. Contour plot of radial velocity.

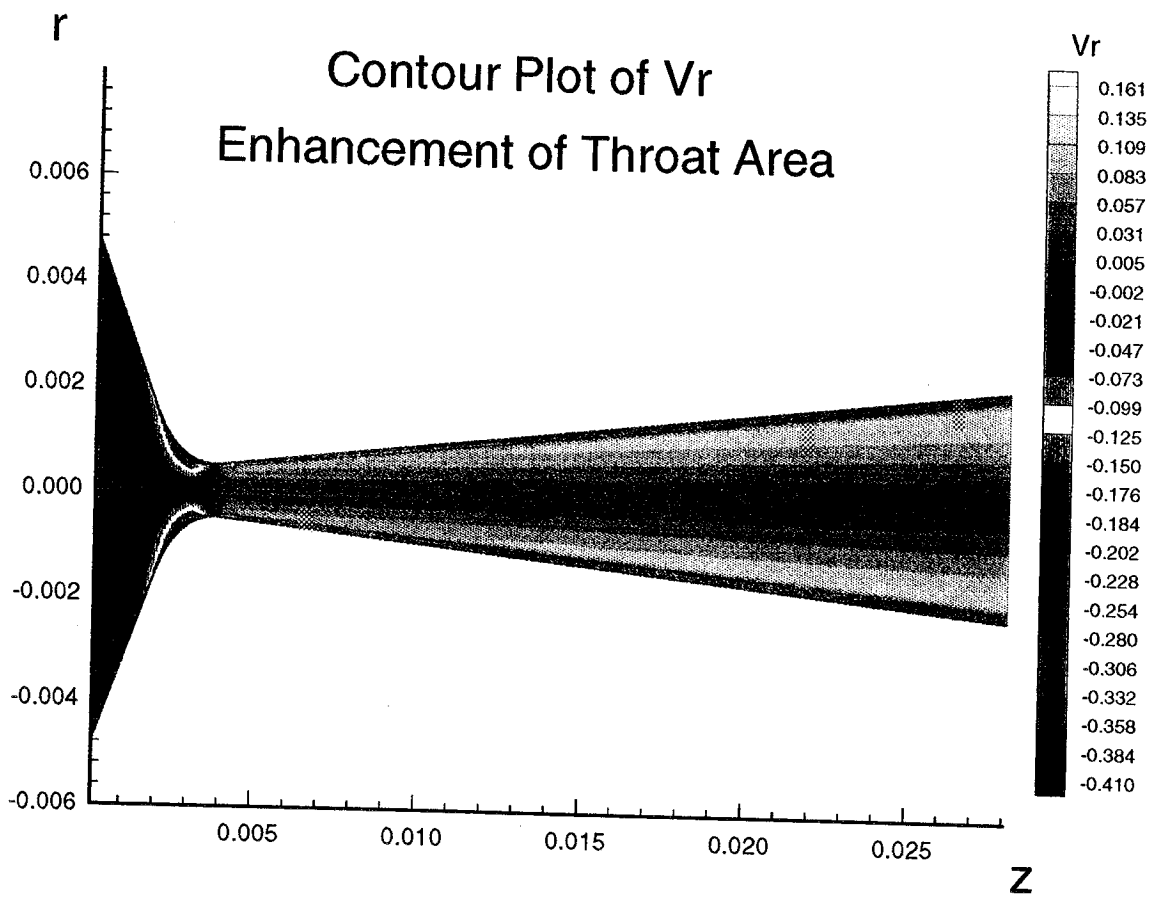

Figure 25. Contour plot of radial velocity.

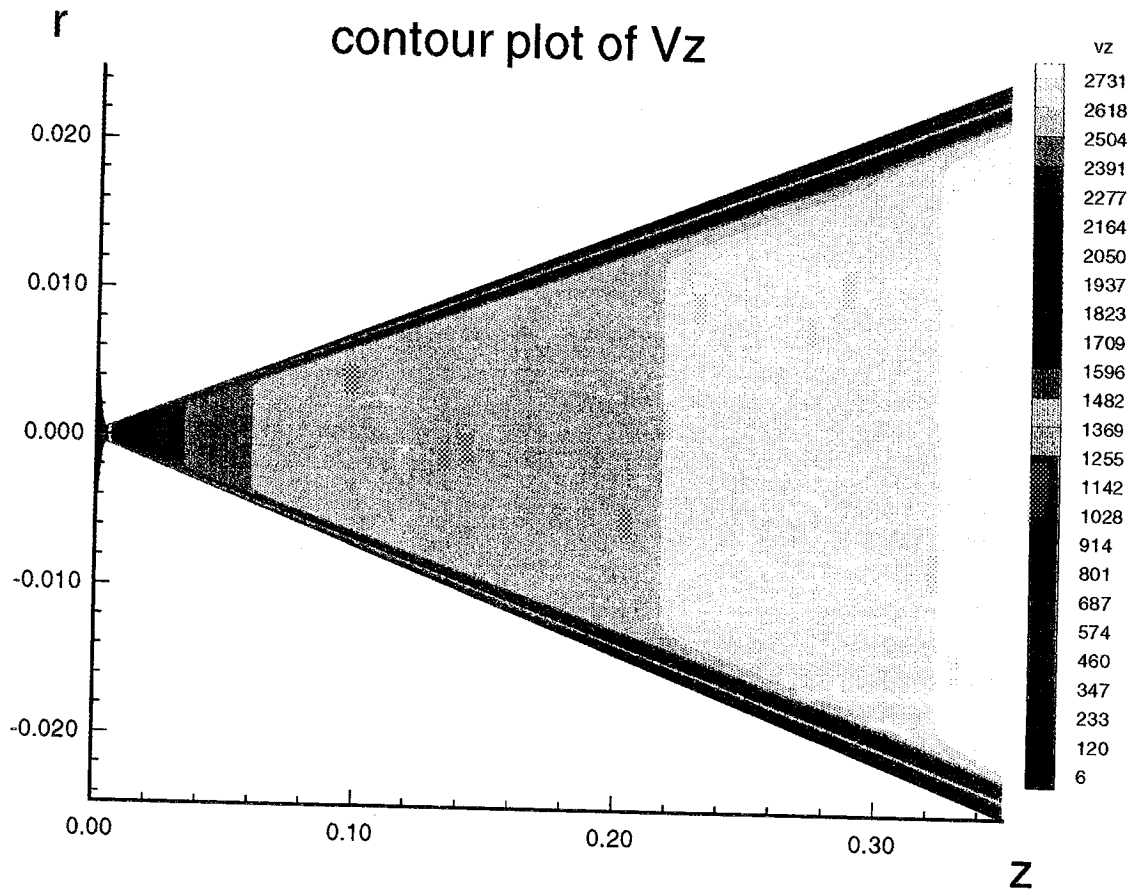

Figure 26. Contour plot of axial velocity.

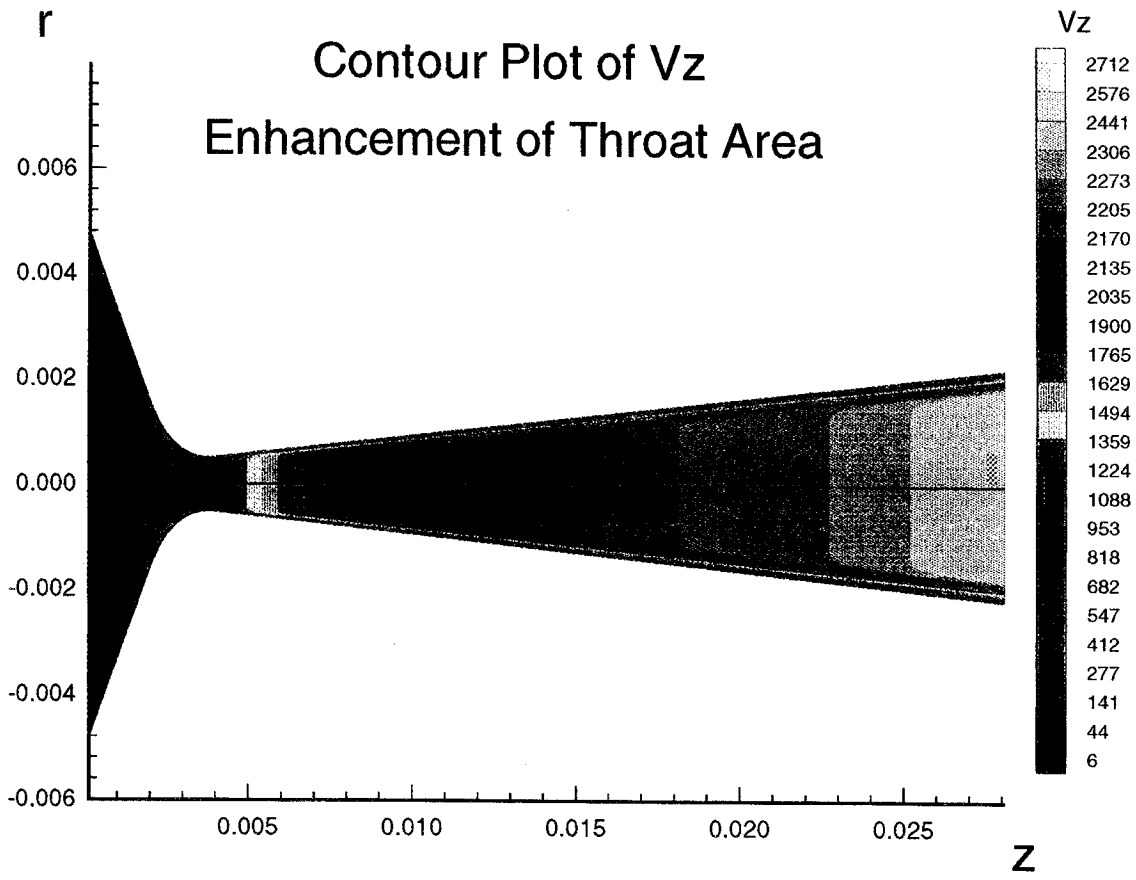

Figure 27. Contour plot of axial velocity.

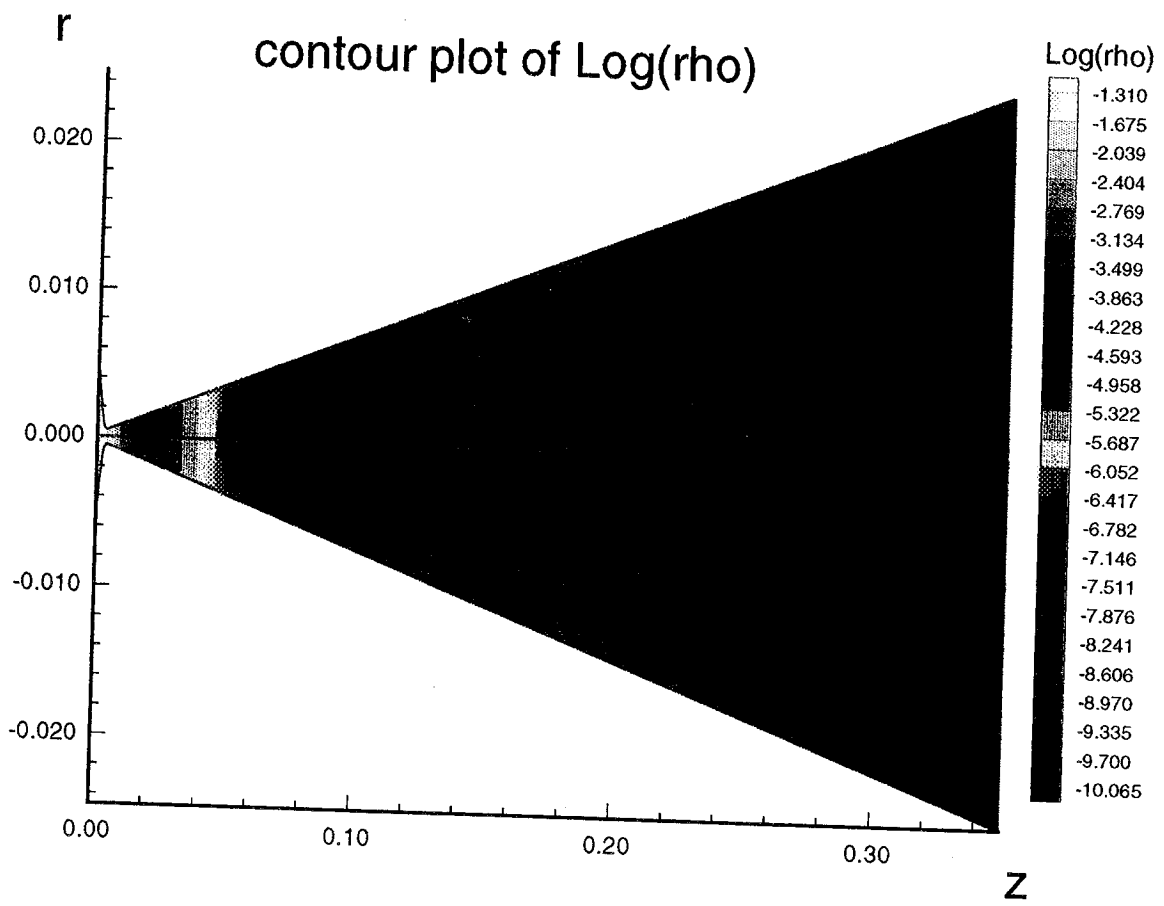

Figure 28. Contour plot of logarithm of density.

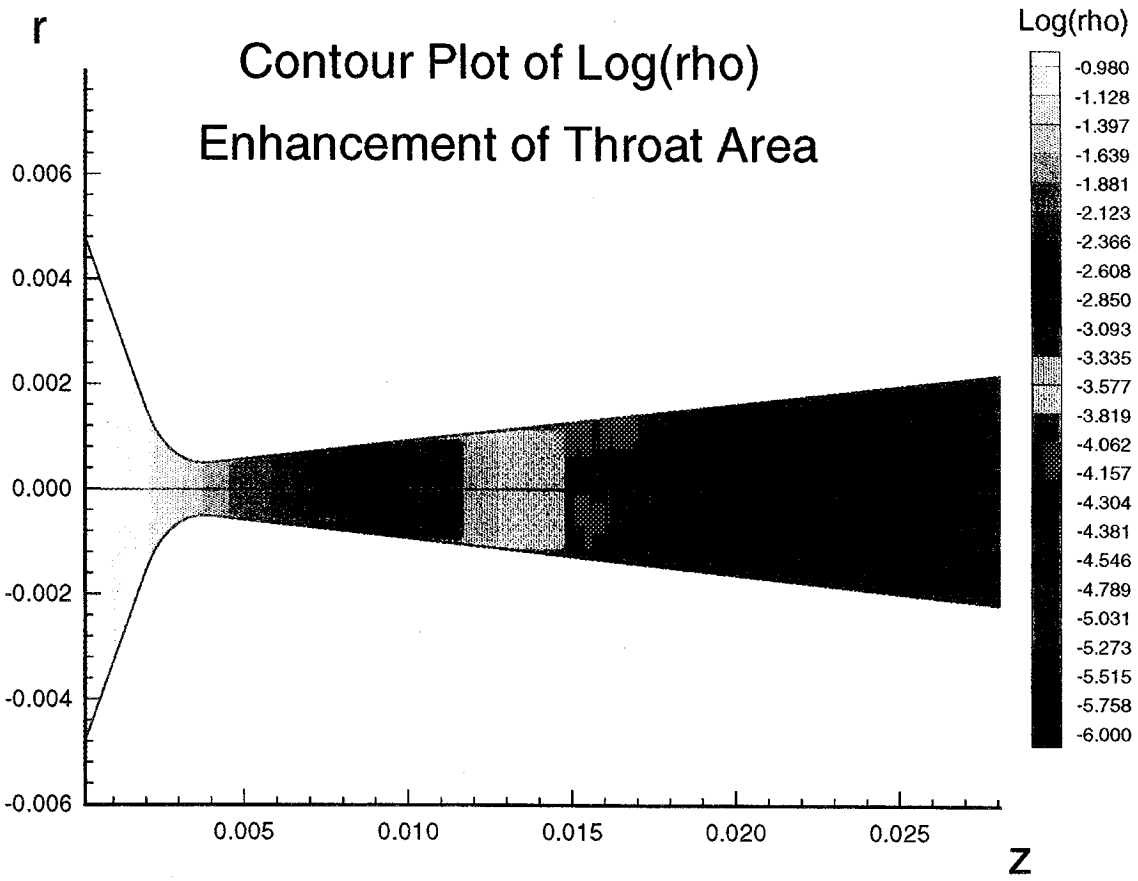

Figure 29. Contour plot of logarithm of density.

Results indicate that the vibrational temperature has essentially a frozen value, along the centerline, upon passage through the throat area into the diverging portion of the nozzle, the same as reported in the references [2],[3]. As the flow expands into the diverging nozzle region, the density of the gas decreases, and the Knudsen number becomes large. Thus, care must be exercised in the nozzle design (Shape of diverging portion of the nozzle) and choice of initial parameters (Inlet pressure) in order that the model remain valid.

In the boundary layer the vibrational temperature is not frozen. These vibrational temperature effects imply that there is no meaning to the term "Mach Number" in this situation as the speed of sound is dependent upon the vibrational properties of the gas. In both models the boundary layer thickness becomes very thin for high Reynolds number flow. A high initial pressure insures both a low Knudsen number and a thin boundary layer. Also, an increased pressure produces a more uniform flow in the nozzle. These results are consistent with those reported in reference [5].

A more detailed analysis of model 2 will be given in Mr. Landry's thesis, which will be an addendum to this report and submitted at a later date.

In conclusion, we have developed two models for the study of high pressure gas flow through nozzles. We have investigated the basic physics associated with the modeling of such a problem under a variety of circumstances. Improved models for gas vibrational relaxation were employed during the analysis. The numerical analysis produced both quantitative and qualitative results associated with both equilibrium and nonequilibrium thermodynamic flow physics through a converging-diverging nozzle. It turns out that these problems are extremely difficult to solve numerically and care should be taken upon the selection of the numerical method employed. They are challenging problems for current and existing numerical techniques. The development of numerical techniques which will handle these types of problems quickly and efficiently are areas for additional research.

APPENDIX A
LIST OF SYMBOLS

a	Speed of Sound $[m/s]$
A	Cross sectional area $[m^2]$
$\vec{b}$	Body force per unit mass $[Newton/Kg]$
C_v, C_{vrt}, V_{vv}	Specific heat at constant volume $[Joule/Kg\,K]$
$D_{i,j}$	Rate of deformation tensor $[s^{-1}]$
$\frac{D}{Dt} = \frac{\partial}{\partial t} + \vec{V} \cdot \nabla$	Material or substantial derivative
e, e_{rt}, e_v	Energy per unit mass $[Joule/Kg]$
e_t	Energy per unit volume $[Joule/m^3]$
$\hbar$	Plank's constant $[Joule\,s]$
h	Enthalpy $[Joule/m^3\,s]$
k	Boltzmann's constant $[Joule/K]$
K, K_{rt}, K_v	Thermal conductivities $[W/m\,K]$
$m = W/N_a$	Molecular mass $[Kg]$
M	Mach number
N_a	Avogadro's number $[mol^{-1}]$
$\vec{q}, \vec{q_{rt}}, \vec{q_v}$	Heat input per unit volume $[Joule/m^3\,s]$
P	Pressure $[Newton/m^2]$
R	Gas Constant $[Joule/Kg\,K]$
r	Radial distance $[m]$
s	Entropy per unit volume $[Joule/m^3\,s\,K]$
t	Time $[s]$
T, T_v	Temperatures $[K]$

$\vec{V}$	Velocity $[m/s]$
V_r, V_z	Velocity components $[m/s]$
W	Molecular weight of N_2 $[Kg]$
X	Coupling term $[K/s]$
x, y	Computational coordinates
z	axial distance $[m]$
η	Viscosity coefficient $[Kg/m\,s]$
λ	Second coefficient of viscosity $[Kg/m\,s]$
ϱ	Density $[Kg/m^3]$
τ	Relaxation time $[s]$
τ_{ij}	Stress tensor $[Newton/m^2]$
ϕ, θ, ξ	Characteristic temperatures $[K]$
ν	Frequency $[s^{-1}]$
$\gamma = \frac{C_p}{C_v}$	Ratio of specific heats

APPENDIX B
NOZZLE DESIGN

The nozzle shape is illustrated in the figure B1 and can be described by a straight line 1 , circle, cubic spline and straight line 2. In this figure $a_0 = 0.5mm$ is the throat radius, $b = 350mm$ is the length of the nozzle, $r_0 = 5.0mm$ is the entrance radius, and $R = 2.0mm$ is the radius of the circle. The parameters a_1, a_2, a_3, a_4 are selected such that the line 1, circle, cubic spline and line 2 are connected in a continuous fashion. We require that at $z = a_1$ that the slope of the line 1 and slope of the circle are equal. At $z = a_2$ the slope of the circle is zero. The parameter a_3 is selected such that the cubic spline converts the circle to the line 2.

We write the equation of the circle as

$$(r - (a_0 + R))^2 + (z - a_2)^2 = R^2 \tag{b1}$$

and the equation of the line 1 as

$$r - 5 = m1 * z \tag{b2}$$

where $m_1 = -\tan(60°)$ is the slope of line 1. The slope at any point on the circle can be determined from the derivative of equation (b1)

$$(r - (a_0 + R))\frac{dr}{dz} + (z - a_2) = 0 \tag{b3}$$

At $z = a_2$ we require that the slope of the circle is zero, $\frac{dr}{dz} = 0$ and at $z = a_1$ we require that the point $z = a_1$,$r = r_1$ lie on both the circle and line 1 so that

$$r_1 - (a_0 + R) = -\sqrt{R^2 - (a_1 - a_0)^2} \tag{b4}$$

and

$$\sqrt{R^2 - (a_1 - a_2)^2} * m_1 = -(a_1 - a_2). \tag{b5}$$

Solving the equation (b4) for $a_1 - a_2$ we find that

$$a_1 - a_2 = -\sqrt{3}R/2. \tag{b6}$$

From the equation (b4) we find

$$r_1 = a_0 + R - \sqrt{R^2 - 3}. \tag{b7}$$

The circle intersects the line 1 at the point (a_1, r_1) which gives the equation of line 1

$$r - (a_0 + R - \sqrt{R^2 - 3}) = m_1 * (z - a_1). \tag{b8}$$

Note that at $z = 0$, where $r = r_0 = 5$ we find that

$$\begin{aligned} & 5 - (a_0 + R - \sqrt{r^2 - 3}) = \sqrt{3} a_1 \\ \text{or} \quad & a_1 = \frac{5 - (a_0 + R - \sqrt{R^2 - 3})}{\sqrt{3}} \end{aligned} \tag{b9}$$

For $0 \leq z \leq a_1$ the nozzle shape is described

$$r = f(z) = m_1 * (z - a_1) + a_0 + R - \sqrt{R^2 - 3} \tag{b10}$$

or

$$r = f(z) = m_1 * (z - a_2) + a_0 + R - 3 - \sqrt{R^2 - 3} \tag{b11}$$

where $m_1 = -\tan(60°) = -\sqrt{3}$. For the region $a_1 \leq z \leq a_2$ the nozzle shape is described

$$r = f(z) = a_0 + R - \sqrt{R^2 - (z - a_2)^2} \tag{b12}$$

For the region $a_2 \leq z \leq a_3$ we must find the parameter a_3 such that the cubic spline converts the circle to the line 2. The cubic spline is represented as

$$r = S_3(z) = A(z - a_2)^3 + B(z - a_2)^2 + C(z - a_2) + D \tag{b13}$$

and is subject to the end conditions

$$\begin{aligned} S_3(a_2) &= a_0 & S_3(a_3) &= a_4 \quad \text{(unknown)} \\ S_3'(a_2) = \frac{dr}{dz}|_{z=a_2} &= 0 & S_3'(a_3) &= m_2 = \tan\theta \quad \text{(slope of line 2)} \\ S_3''(a_2) &= \frac{1}{R} & S_3''(a_3) &= 0 \end{aligned}$$

Solving this system of equations we find

$$A = \frac{-1}{12R^2 m_2} \qquad B = \frac{1}{2R} \qquad C = 0 \qquad D = a_0 \tag{b14}$$

and consequently

$$a_3 = a_2 + 2Rm_2, \qquad a_4 = S_3(a_3) = a_0 + 4Rm_2^2/3 \tag{b15}$$

Then the nozzle shape for the region $a_2 \leq z \leq a_3$ is given by

$$r = f(z) = \frac{-(z-a_2)^3}{12R^2 m_2} + \frac{(z-a_2)^2}{2R} + a_0 \qquad (b16)$$

and for the region $a_3 \leq z \leq b$ we have

$$r = f(z) = a_4 + m_2 * (z - a_3). \qquad (b17)$$

The equations (b10),(b12),(b16) and (b17) must be converted from millimeters to meters for use in our analysis.

In summary, for r in meters, z in millimeters and using the conversion factor $cv = 10^{-3}$, the equations describing the shape of the nozzle can be written

$$\begin{aligned}
0 \leq z \leq a_1, \quad & r = f(z) = cv * (m_1 * (z - a_2) - a_0 + R - 3 - \sqrt{R^2 - 3}) \\
a_1 \leq z \leq a_2, \quad & r = f(z) = cv * (a_0 + R - \sqrt{R^2 - (z-a_2)^2}) \\
a_2 \leq z \leq a_3, \quad & r = f(z) = cv * (\frac{-(z-a_2)^3}{12R^2 m_2} + \frac{(z-a_2)^2}{2R} + a_0) \\
a_3 \leq z \leq b, \quad & r = f(z) = cv * (a_4 + m_2 * (z - a_3))
\end{aligned}$$

where

$$\begin{aligned}
m_1 &= -\tan 60^\circ & a_1 &= \frac{5 - a_0 - R + \sqrt{R^2 - 3}}{\sqrt{3}} \\
m_2 &= \tan\theta & a_2 &= a_1 + \sqrt{3}R/2 \\
\theta &= 4^\circ & a_3 &= a_2 + 2Rm_2 \\
a_0 &= 0.5\,mm & a_4 &= a_0 + \frac{4Rm_2^2}{3} \\
R &= 2.0\,mm & & \\
r_0 &= 5.0\,mm & &
\end{aligned}$$

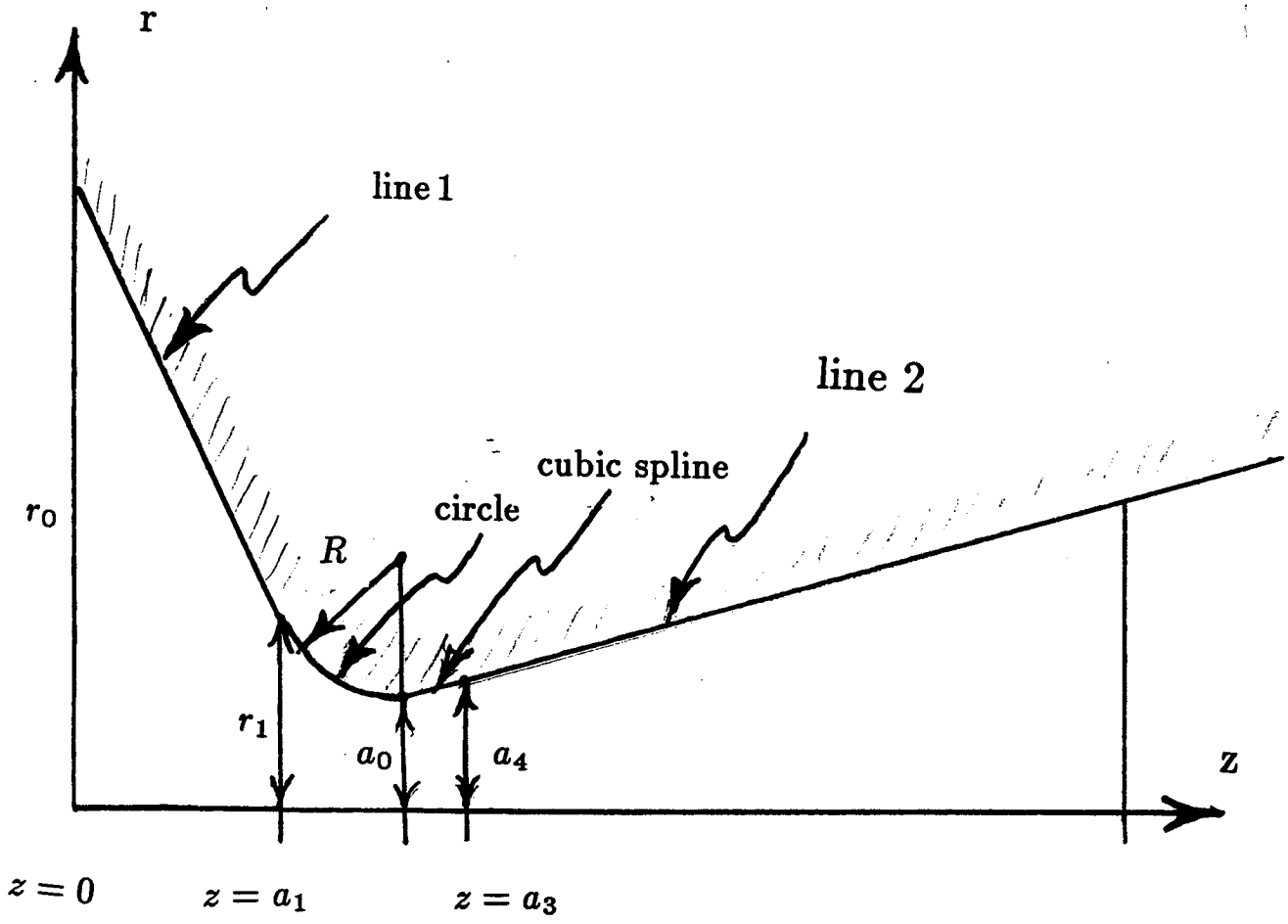

Figure B1 Nozzle Shape

REFERENCES

1. R.W. MacCormack, "Current Status of Numerical Solutions of the Navier-Stokes Equations", AIAA 23rd Aerospace Sciences Meeting, AIAA-85-0032, Jan, 1985.
2. Tahir Gökçen, "Computation of Nonequilibrium Viscous Flows in Arc-Jet Wind Tunnel Nozzles", 32nd Aerospace Sciences Meeting, AIAA-94-0254, Jan. 1994.
3. P.A. Gnoffo, "Application of Program Laura to Thermochemical nonequilibrium Flow through a nozzle", Hypersonic Flows for Reentry Problems, Vol.2, Springer-Verlag, 1991, Pp.1145-1158.
4. J.J. Korte, A. Kumar, D.J. Singh, B. Grossman, "Least Squares/Parabolized Navier-Stokes Procedure for Optimizing Hypersonic Wind Tunnels Nozzles", AIAA/SAE/ASME 27th joint Propulsion Conference, AIAA-91-2273, June 1991.
5. J.J. Korte, E. Hedlund, S. Anandakrishnan, "A comparison of Experimental data with CFD for NSWC Hypervelocity Wind Tunnel #9 Mach 14 Nozzle", AIAA 17th Aerospace Ground Testing Conference, AIAA-92-4010, July 1992.
6. J.J. Korte, "An Explicit Upwind Algorithm for Solving the Parabolized Navier-Stokes Equations", NASA Technical Paper 3050, February 1991.
7. W.E. Meader, G.A. Miner, J.H. Heinbockel, "Vibrational Relaxation in Hypersonic Flow Fields", NASA Technical Paper 3367, Sept. 1993.
8. H.E. Bailey, R.M. Beam, "Newton's Method Applied to Finite-Difference Approximations for the Steady-State Compressible Navier-Stokes Equations", Journal of Computational Physics, 93, 108-127, 1991.
9. P.D. Thomas, "Boundary Conditions for Implicit Solutions to the Compressible Navier-Stokes Equations in Finite Computational Domains", AIAA Computational Fluid Dynamics Conference, AIAA 79-1447, July, 1979, Williamsburg, Va.
10. S. Parameswaran, I. Kiris, "A Steady, Shock-Capturing Pressure-Based Computational Procedure for Inviscid, Two-Dimensional Transonic Flows", Numerical Heat Transfer, Part B, Vol 23, Pp221-236, 1993.
11. S. Parameswaran, "Steady, Shock-Capturing Method Applied to One-Dimensional Nozzle Flow", AIAA Journal, Vol 27, No. 9, Pp1292-1295.
12. N.L. Rapagnani, F.R. Sumpano, "Theoretical and Experimental Description for a Radial Supersonic Flowfield", AIAA Journal, Now, Vol. 24, 1986.

13. R.P. Benedict, *Fundamentals of Gas Dynamics*, John Wiley and Sons, Inc., 1983.

14. D.A. Anderson, J.C. Tannehill, R.H. Pletcher, Computational Fluid Mechanics and Heat Transfer, Hemisphere Publishing Co., 1984.

15. G.A. Hasen, "Navier-Stokes Solutions for a Supersonic Coflowing Axis-symmetric Nozzle with a Thick Base Annulus", Ph.D. Thesis, Air Force Institute of Technology, 1981. University Microfilms #8119138.

16. M.R. LaPointe, "Numerical Simulation of Self-Field MPD Thrusters", AIAA/SAE/ASME/ASEE 27th Joint Propulsion Conference, AIAA 91-2341, June, 1991.

17. J.S. Shang, "An Assessment of Numerical Solutions of the Compressible Navier-Stokes Equations, AIAA 17th Fluid Dynamics, Plasma Dynamics and Lasers Conference, AIAA 84-1549, June 1984.

18. P. Canupp, G. Candler, J.Perkins and W. Erikson, "Analysis of Hypersonic Nozzles Including Vibrational Nonequilibrium and Intermolecular Force Effects", 30th Aerospace Sciences Meeting, AIAA 92-0330, January 1992.

19. S.S. Penner, *Thermodynamics for Scientists and Engineers* , Addison-Wesley Publishing Co., 1968.

20. G.A. Hasen, "Navier-Stokes Solutions for an Axisymmetric Nozzle", AIAA/SAE/ASME 17th Joint Propulsion Conference, AIAA 81-1494, July 1981.

21. J.A. Hatfield, G.V. Candler, "Examination of Nonequilibrium Effects in an Ionized Nitrogen Flow", AIAA 31st Aerospace Sciences Meeting, AIAA 93-0478, January 1993.

22. D.B. Landrum, G.V. Candler, "Development of a New Model for Vibration Dissociation Coupling in Nitrogen", AIAA 27th Thermophysics Conference, AIAA 92-2853, July 1992.

23. E. von Lavante, A. Haertl, D. Claes, Numerical Solutions of Euler Equations Using Simplified Flux Vector Splitting, AIAA/SAE/ASME/ASEE 21st Joint Propulsion Conference, Monterey, CA, July 8-10, 1985.

24. R.M. Beam, R.F. Warming, An Implicit Factored Scheme for the Compressible Navier-Stokes Equations, AIAA Journal, Vol. 16, No. 4, April 1978.

25. J.L. Steger and R.F. Warming, Flux Vector Splitting of the Inviscid Gasdynamic Equations with Applications to Finite-Difference Methods., Journal of Computational Physics 40, 263-293, 1981.

26. W. Kauzmann, *Kinetic Theory of Gases*, W. A. Benjamin, Inc., 1966.

27. K.A. Hoffman, S.T. Chang, *Computational Fluid Dynamics for Engineers*, Vol 1. and Vol. 2, Engineering Education System, Wichita, Kansas, 1993.

28. W.E. Meador, M.D. Williams, G.A. Miner, "Scaling of Vibrational Relaxation in Nitrogen Gases", (Submitted for NASA Technical Report), March 1995.

29. G. A. Bird, "Direct Simulation of Gas Flows at the Molecular Level", Communications in Applied Numerical Methods, Vol. 4, 165-172, 1988.

30. J.O. Hirschfield, C.F. Curtis, R.B. Bird, *Molecular Theory of Gases and Solids* , John Wiley and Sons, 1954.

31. K. Stewartson, "The Theory of Laminar Boundary Layer in Computational Fluids", Oxford, 1964.